



University of
Massachusetts
Amherst

Identification and Functional Characterization of the Zebrafish Gene Quetschkommode (que)

Item Type	Dissertation (Open Access)
Authors	Friedrich, Timo
DOI	10.7275/rsst-tp91
Download date	2026-03-10 13:31:19
Link to Item	https://hdl.handle.net/20.500.14394/39083

**IDENTIFICATION AND FUNCTIONAL CHARACTERIZATION OF THE
ZEBRAFISH GENE *QUETSCHKOMMODE* (*que*)**

A Dissertation Presented

by

TIMO FRIEDRICH

University of Massachusetts Amherst in partial fulfillment of the
requirements for the degree of

DOCTOR OF PHILOSOPHY

September 2012

Molecular and Cellular Biology

© Copyright by Timo Friedrich 2012

All Rights Reserved

**IDENTIFICATION AND FUNCTIONAL CHARACTERIZATION OF THE
ZEBRAFISH GENE *QUETSCHKOMMODE* (*que*)**

A Dissertation Presented

by

TIMO FRIEDRICH

Approved as to style and content by:

Gerald B. Downes, Chair

Rolf O. Karlstrom, Member

Wei-Lih Lee, Member

James Chambers, Member

Dominique Alfandari, Program Director

Molecular and Cellular Biology

ACKNOWLEDGEMENTS

This work would not have come to existence without the help and support of others. First and foremost I would like to thank my advisor, Dr. Gerald Downes for being an excellent mentor, for his time and patience as well as his guidance during all stages of this project. I feel honored to have worked in an extremely supportive and enjoyable atmosphere with great lab members, an extremely helpful zebrafish and UMass community, especially Kelly Anne McKeown, Bryan Olson and Ayse (Tuba) Ozacar for their help during the years and for proofreading the manuscript. I owe much to my family, an invaluable source of support and encouragement during the past 30 years. I also want to thank Tom Galvin and Greg Black for the gift of free flight which kept me soaring even during difficult times as well as the many pilots I had the honor to fly with, teaching me to navigate the skies.

ABSTRACT

IDENTIFICATION AND FUNCTIONAL CHARACTERIZATION OF THE ZEBRAFISH GENE *QUETSCHKOMMODE* (*que*)

SEPTEMBER 2012

TIMO FRIEDRICH, B.S., UNIVERSITÄT KONSTANZ, KONSTANZ

Ph.D., UNIVERSITY OF MASSACHUSETTS AMHERST

Directed by: Professor Gerald B. Downes

Locomotion in vertebrates depends on proper formation and maintenance of neuronal networks in the hind-brain and spinal cord. Malformation or loss of factors required for proper maintenance of these networks can lead to severe neurodegenerative diseases limiting or preventing locomotion. A powerful tool to investigate the genetic and cellular requirements for development and/or maintenance of these networks is a collection of zebrafish mutants with defects in motility. The zebrafish mutant *quetschkommode* (*que*) harbors a previously unknown gene defect leading to abnormal locomotor behavior. Here I show that the *que* mutants display a seizure-like behavior starting around four days post fertilization (dpf) that is characterized by a lack of an initial high amplitude body bend (C-bend) and simultaneous contra-lateral contractions leading to a seizure-like phenotype and paralysis. Peripheral nerve recordings show a significant increase in the number of initiated swimming bouts and overlap between left and right motor neuron activity. These data suggest that the *que* mutation leads to defects

in nervous system function, at the level of motor neurons or central control of motor neurons. I have genetically mapped the *que* locus to a 0.36cM interval on chromosome 22 using meiotic mapping. I identified a splice mutation in the gene ‘dihydrolipoamide branched-chain transacylase E2’ (*dbt*) as defective in *que*. An orthologous mutation in humans leads to Maple Syrup Urine Disease (MSUD), a devastating metabolic disorder leading to seizures, mental retardation, coma and neonatal death if untreated. In zebrafish, *dbt* is expressed throughout early development and *dbt* transcripts become enriched in the hind-brain as well as in the gut and liver by 96 hpf. In MSUD patients levels of branched chain amino acids (BCAA) and their keto acids are significantly increased due to the essential role of the DBT enzyme for the BCAA metabolic pathway. The *que* mutation causes a significant increase of branched chain amino acids in the zebrafish mutant and a strong decrease of neurotransmitters such as glutamate and GABA as well as precursors like glutamine. I hypothesize that reduced neurotransmitter levels in *que* mutants lead to the observed motility phenotype. Consistent with this hypothesis, I show a tissue specific reduction of glutamate in the hind-brain and spinal cord of *que* mutants. To evaluate the *que* mutant’s potential as a vertebrate model for MSUD I performed a pilot drug screen using a selection of metabolites of the pathway as well as diet additives currently evaluated in clinical trials. Conversely, application of phenylbutyrate, one of the diet additives, increased the swimming performance of *que* mutant embryos, while the keto acid α -ketoisocaproate (KIC), one of the elevated keto acids in human patients, decreased the percentage of larvae capable of swimming. These results help establish the zebrafish *que* mutant as a new model for MSUD disease that can be used to further the understanding of this disorder and to help identify therapeutic agents.

TABLE OF CONTENTS

	Page
ACKNOWLEDGEMENTS	iv
ABSTRACT	v
LIST OF TABLES	xi
LIST OF FIGURES	xii
CHAPTER	
1. BACKGROUND AND INTRODUCTION	1
1.1 Introduction	1
1.2 Zebrafish as a model system	2
1.3 Motility mutants as a tool to study neuronal network function	3
1.4 <i>que</i> mutants belong to the accordion class of motility mutants	4
1.5 Maple syrup urine disease (MSUD)	5
1.6 Metabolism in MSUD	7
1.7 Model systems for MSUD	8
1.8 Effects of elevated BCAA levels on the nervous system	8
1.9 Significance	9
2. BEHAVIORAL AND ELECTROPHYSIOLOGICAL CHARACTERIZATION OF THE <i>QUE</i> MUTANT	13
2.1 Abstract	13
2.2 Introduction	14

2.3 Materials and Methods.....	15
2.3.1 Behavioral Analysis.....	15
2.3.2 Antibody staining.....	16
2.3.3 Electrophysiology.....	16
2.4 Results and Discussion.....	17
2.4.1 <i>que</i> mutants exhibit abnormal rostrocaudal compressions in response to touch.....	17
2.4.2 <i>que</i> mutants do not exhibit gross muscle or nerve structure defects.....	18
2.4.3 <i>que</i> mutants demonstrate abnormal CNS motor output.....	19
2.4.4 Significance.....	20
3. MOLECULAR IDENTIFICATION OF THE <i>QUE</i> LOCUS.....	26
3.1 Abstract.....	26
3.2 Introduction.....	26
3.3 Methods.....	27
3.3.1 Chromosomal mapping and sequence analysis.....	27
3.3.2 Morpholino analysis.....	27
3.4 Results and Discussion.....	28
3.4.1 Chromosomal mapping and sequence analysis.....	28
3.4.2 Confirmation through phenocopying.....	29

3.5 Significance.....	30
4. FUNCTIONAL CHARACTERIZATION OF THE DIHYDROLIPOAMIDE BRANCH CHAIN TRANSACYLASE E2 GENE.....	35
4.1 Abstract.....	35
4.2 Introduction.....	35
4.3 Methods.....	36
4.3.1 RT-PCR.....	36
4.3.2 Whole-mount in situ hybridization	37
4.3.3 Western Blot Analysis	37
4.3.4 Amino Acid Quantification.....	38
4.3.5 Immunohistochemistry	38
4.3.6 Pharmacological approach	39
4.4 Results and Discussion	40
4.4.1 <i>dbt</i> mRNA becomes enriched in the brain and gut organs during development	40
4.4.2 <i>que</i> mutants harbor elevated levels of BCAAs	41
4.4.3 Glutamate levels are reduced in the brain of <i>que</i> mutant larvae.....	42
4.4.4 The working model	43
4.4.5 Pharmacological evaluation of the working model	44
4.5 Significance.....	46

5. SUMMARY AND FUTURE DIRECTIONS	59
5.1 <i>que</i> mutants as a zebrafish model for MSUD	60
5.2 Future directions	61
5.2.1 The role of Glutamate and neurotransmitter reduction	61
5.2.2 Screening for therapeutic compounds.....	62
5.2.3 Tissue specific rescue	63
5.2.4 The pathway from BCAAs to the phenotype.....	65
APPENDIX: A MACONDO CRUDE OIL FROM THE DEEPWATER HORIZON OIL SPILL DISRUPTS SPECIFIC DEVELOPMENTAL PROCESSES DURING ZEBRAFISH EMBRYOGENESIS	66
REFERENCES	70

LIST OF TABLES

Table	Page
1.1 Accordion class mutants	10
2.1 Comparison of bout and burst properties related to fictive locomotor activity in wild Type and <i>que</i> mutants	25
4.1 Compounds and concentrations used for pharmacological pilot screen	55

LIST OF FIGURES

Figure	Page
1.1 Branched Chain Amino Acid Metabolism.....	11
1.2 Model for regulation of Branched Chain Amino Acids in mitochondria	12
2.1 <i>que</i> mutants exhibit abnormal swimming behavior at 96 hpf.....	21
2.2 <i>que</i> mutants do not exhibit gross nerve or muscle structure defects.....	23
2.3 The spinal locomotor output is altered in <i>que</i> mutants	24
3.1 Protein sequence alignment of human and zebrafish <i>dbt</i>	31
3.2 The <i>que</i> gene encodes dihydrolipoamide branched-chain transacylase E2 (<i>dbt</i>), a subunit of the BCKD complex.....	32
3.3 <i>dbt</i> morpholino decreases <i>dbt</i> protein levels.....	34
4.1 <i>dbt</i> becomes enriched in the brain and organs in the gut across development	48
4.2 <i>dbt</i> protein expression during development.....	49
4.3 The free amino acid profile of <i>que</i> mutants shows elevated levels of BCAAs at 96 hpf.....	50
4.4 <i>que</i> mutants contain a reduced concentration of glutamate in the brain.	51
4.5 Levels of Glutamate during development.....	53
4.6 A working model of how mutation of <i>dbt</i> results in abnormal, accordion behavior.....	54
4.7 Bull's Eye for kinematic analysis	56
4.8 Pharmacological evaluation of the model.....	57
A.1 Macondo crude oil exposure impaired escape behavior by 48 hpf.....	69

CHAPTER 1

BACKGROUND AND INTRODUCTION

1.1 Introduction

Locomotion in vertebrates depends on proper formation and maintenance of neuronal networks in the hindbrain and spinal cord. Malformation or loss of factors required for the function of these networks can lead to severe neurodegenerative diseases limiting or preventing locomotion. The zebrafish mutant *quetschkommode* (*que*) demonstrates abnormal seizure-like motor behavior (Granato et al. 1996). Previous to this work, the mutation underlying the *que* phenotype had not been determined nor had its behavior been characterized in detail. Wild-type larvae respond to touch stimuli to the head at 4 days post fertilization (dpf) with a high amplitude body bend with the tip of the tail touching the head (C-Bend) followed by alternating body bends propelling the larvae away from the direction of the stimulus. While being indistinguishable from wild-type siblings until after 3 dpf *que* mutants mostly fail to perform C-bends, compress rostrocaudally and remain in this seizure-like state until the end of the response with only minimal, mostly uncoordinated tail movements. In this dissertation I have compared the tail angle of *que* mutants to known muscle and central nervous system (CNS) defect mutants and use peripheral nerve recordings to determine whether *que* mutants harbor a neurological or muscle defect as described in Chapter 2. In Chapter 3, the mutation was determined and found that the mutated gene has implications for Maple Syrup Urine Disease (MSUD), a human metabolic disorder. I characterized the metabolic criteria such

as severe changes in free amino acid and neurotransmitter levels (Chapter 4). Part of this characterization was also a pilot drug screen with the intention of testing a working model of how the *que* gene leads to the observed locomotor defect as well as testing the feasibility of using the *que* mutant as a tool to screen small compound libraries for new potential drugs to treat MSUD.

1.2 Zebrafish as a model system

Zebrafish as a model system to study vertebrate development has many key advantages and benefits. First, during the initial five days post fertilization the neuronal networks responsible for locomotion go through several stages of development characterized by increasing complexity. During this transition the embryos and larvae display various discrete motor phenotypes during early development such as spontaneous movement after 17hpf, touch evoked tail coiling after 21hpf and escape responses after 27hpf (Granato et al. 1996; McKeown et al. 2012). These defined behaviors can be used to find new genes required for neuronal network formation by mapping chemically induced mutations in mutants displaying motility defects (Granato et al. 1996; Haffter et al. 1996; Downes and Granato 2004; Gleason et al. 2004; Hirata et al. 2005; Olson, Sgourdou, and Downes 2010; McKeown et al. 2012). Second, maintenance of many different transgenic lines is relatively inexpensive. Third, embryos develop externally and most organ systems are formed at 5 dpf. This rapid development as well as the initial transparency of the embryo makes zebrafish highly amenable to optical methods. Forth, a great variety of genetic tools and resources are shared among the research community. Among these resources are mutant collections obtained from insertional mutagenesis

(Amsterdam et al. 1999) or N-ethyl-N-nitrosourea (ENU) mutagenesis screens (Granato et al. 1996).

Zebrafish mutants have been used for forward genetics to search for genes involved in many aspects of development such as cardiac muscle formation (Langenbacher et al. 2011) and eye development (Tschopp et al. 2010) but also for seeking novel genes involved in seizure resistance (Baraban et al. 2007) and in neuronal network formation (Wolman and Granato 2012). Mapping of these mutants is facilitated by a sequenced zebrafish genome and extensive polymorphism databases available online. Fifth, knockdown strategies using antisense morpholino oligomers, which are injected at the 1-4 cell stage, can be used to knock down translation of specific transcripts of interest (Bill et al. 2009; McKeown et al. 2012). Lastly, the aquatic habitat facilitates pharmacological approaches and screens; most water soluble compounds can simply be applied to the external embryo medium (Parng et al. 2002; Hao et al. 2010; Zhong and Lin 2011). Taken together, these benefits make zebrafish an excellent model to study genes and factors involved in the development of locomotion.

1.3 Motility mutants as a tool to study neuronal network function

In a large scale mutagenesis screen zebrafish were exposed to the mutagen ENU. After outcrossing multiple mutations the offspring were analyzed for developmental and behavioral defects. This experiment yielded a large collection of mutants with various phenotypes of abnormal locomotion (Granato et al. 1996). The 166 obtained mutants, that together contain around 48 genes, fall into 14 phenotypic groups. The 8 mutants of the accordion group respond to touch at 24 hpf with rostrocaudal compression and were

therefore grouped together due to the similarity to the musical instrument (Table 1.1). Initially most accordion class mutants were thought to be in the glycinergic pathway due to the observation that application of glycine receptor agonist strychnine can cause an accordion-like phenotype (Downes and Granato 2006). The mutant *bandoneon* (*beo*) has been found to harbor a defect in the glycine receptor β -subunit (Hirata et al. 2005). Despite this example for a CNS defect in accordion class mutants most mutants seem to be affected by impaired muscle relaxation (Gleason et al. 2004; Hirata et al. 2004; Olson, Sgourdou, and Downes 2010) or a defect at the neuromuscular synapses (Downes and Granato 2004; Lefebvre et al. 2004; M. Wang, Wen, and Brehm 2008). Most mapped mutants have turned out to have implications for human diseases and have contributed to the understanding of the signaling pathways underlying the symptoms (Downes and Granato 2004; Gleason et al. 2004; Hirata et al. 2004; Hirata et al. 2005; Lefebvre et al. 2004; M. Wang, Wen, and Brehm 2008; Olson, Sgourdou, and Downes 2010; McKeown et al. 2012).

1.4 *que* mutants belong to the accordion class of motility mutants

quetschkommode (*que*) is an autosomal recessive mutation of the accordion class generated in a large-scale ENU screen (Granato et al. 1996). The onset of the phenotype was initially been described as 24-28 hpf (Granato et al. 1996) but the onset of the behavior may depend on the genetic background and could be variable. In our mixed toplongfin-tubingen (TLF-TU) background *que* mutants display normal spontaneous tail coiling behavior at 17 hpf and are capable of touch evoked swimming at 21 hpf. After 72 hpf, the mutant larvae gradually cease to respond with an initial high amplitude body bend also lacking the rhythmic tail movements and instead become increasingly

paralyzed at 96 hpf. At this time homozygous mutants respond to touch with rostrocaudal compression. This characteristic reaction is thought to be caused by simultaneous long lasting contra-lateral muscle activation followed by uncoordinated seizure-like behavior characterized by uncoordinated arrhythmic body bends. While *que* mutants demonstrate robust accordion behavior their phenotype was not characterized in detail. In 2007 Geisler and colleagues mapped several of these mutants as a service to the community and linked the *que* mutation to chromosome 22 leaving the locus of the mutation still to be determined (Geisler et al. 2007). At the inception of this thesis it was not known whether the *que* mutation affects locomotion through the central nervous system (CNS), primarily at the muscle or through other mechanisms and if homologous mutations have been found in humans leading to similar impairment of locomotion.

1.5 Maple syrup urine disease (MSUD)

Proper neuronal network function and locomotion depend on the presence of all network components, as well as a controlled environment that allows for proper cellular metabolism. In Maple Syrup Urine Disease (MSUD) neuronal networks experience a severe increase of branched chain amino acids (BCAA) such as leucine isoleucine and valine, leading to severe states of metabolic crisis including seizure, coma and death (Kevin A. Strauss and Morton 2003; Chuang, Chuang, and Wynn 2006; Chuang, D. T., Wynn, R. M. and Shih, V. E. 2008; Zinnanti et al. 2009; Zinnanti and Lazovic 2012). On average up to 100,000 children are affected worldwide (Mackenzie and Woolf 1959) but due to founder effects the rate can be as high as 1:200 children in Old Order Mennonite communities (Morton et al. 2002). The increased levels of BCAAs are thought to be compensated by the mother's metabolism until birth. After birth BCAA levels quickly

rise and result in a burnt sugar smell of bodily secretions. A few days after birth, abnormalities in behavior such as repetitive movements like fencing and bicycling can occur followed by seizures, coma and death if untreated (Kevin A. Strauss and Morton 2003). The impaired locomotion is not limited to neonatal stages but can also be triggered by severe metabolic shocks in adults.

The extent of the MSUD phenotype in patients depends on the amount of residual enzyme activity which has been used to separate MSUD disease variants. A residual enzyme activity of 0-2% with an onset at birth and severe myelination failure, coma and death is considered the classic variant (cMSUD) (Ogier de Baulny and Saudubray 2002; Chuang, D. T., Wynn, R. M. and Shih, V. E. 2008). Intermittent (iMSUD) and Intermediate MSUD are considered an enzyme activity of 5-20% with an onset between 0.5-5 years or juvenile stage respectively, both leading to neurological and growth impairment as well as seizures (Chuang, D. T., Wynn, R. M. and Shih, V. E. 2008; K J Skvorak 2009). A subset of mutations in the E2 subunit (discussed in the next chapter) has been shown to respond to thiamine with increased enzyme activity and can be considered a variant with 2-40% enzyme activity and a late, juvenile onset and a phenotype similar to iMSUD (Danner et al. 1985; Fernhoff et al. 1985; Fisher et al. 1991).

Treatment consists of a lifelong diet with reduced amounts of BCAAs adjusted to stabilize the BCAA levels in the blood to normal levels. Despite the constant adjustment unforeseen events such as sickness or injury can cause a metabolic imbalance and shock which can lead to neurological damage (Kevin A Strauss et al. 2010). A second option is a liver transplantation followed by lifelong immunosuppression.

1.6 Metabolism in MSUD

One key metabolic pathway for the digestion of protein is the BCAA degradation (Figure 1.1). It converts BCAAs like leucine, isoleucine and valine to CoA conjugates required for anabolic processes such as neurotransmitter synthesis, energy generation by providing substrates for the Krebs cycle as well as to ensure an osmotic equilibrium in the brain through the control of free amino acids (Chuang, D. T., Wynn, R. M. and Shih, V. E. 2008; Kevin A Strauss et al. 2010; Knerr et al. 2012). In a first reversible step, the BCAAs are converted into their respective keto acids (BCKA) by several aminotransferases in the cytoplasm and mitochondria. The second step is an oxidative decarboxylation of the α -keto acids by the mitochondrial branched chain α -keto dehydrogenase (BCKD) complex. Multiple enzymes form the BCKD complex (Figure 1.2). The E2 subunit functions as transacylase and forms a cubic core as a homo-24-mer (Chuang, D. T., Wynn, R. M. and Shih, V. E. 2008; Zinnanti and Lazovic 2012). It is surrounded by 12 E1 heteromers consisting of α 2 and β 2 subunits. In addition the E2 core has six E3 homodimers attached to it which function as dehydrogenases. Its activity is regulated by the BCKD kinase and phosphatase through phosphorylation of the E1 subunit (Danner and Doering 1998). Mutation in any of the 4 genes coding for the BCKD complex can lead to MSUD. Mutations in the E1 and E2 subunit lead to classic or intermediate MSUD depending on the residual enzyme activity (Chuang, D. T., Wynn, R. M. and Shih, V. E. 2008). Mutation in the E3 subunit involves lactic acidosis as well as elevated BCAAs since the E3 subunit is shared with the α -ketoglutarate and pyruvate dehydrogenases (Chuang, Chuang, and Wynn 2006; Chuang, D. T., Wynn, R. M. and

Shih, V. E. 2008). The sweet smell noticed on bodily secretions is due to the high concentrations of the keto acid form of isoleucine: α -keto- β -methylvalerate (KMV).

1.7 Model systems for MSUD

Historically MSUD has been primarily been studied in bovine and rodent models (K J Skvorak 2009). Calves of the bovine models were mostly stillborn or die quickly after birth. In addition the high cost, the difficulties of handling the animals as well as inconsistencies when compared to human MSUD made the calve model less attractive as a model system (Harper et al. 1989). Several mouse models have been created through mutations in the Branched Chain Amino Acid Transferase in the mitochondria (BCATm) as well as the E2 and E3 subunits. But no reported mutations in BCATm in humans as well as a homozygous embryonic lethality not reflecting human pathology reduced the usefulness of these models (Klivenyi et al. 2004; Calingasan et al. 2008; K J Skvorak 2009). To overcome these drawbacks a classic mouse model was generated through knockout of the E2 subunit (Homanics et al. 2006). On top of this background, human E2 was expressed by a liver specific promoter resulting in 5-6% of normal enzyme activity (Homanics et al. 2006). This increased the survival rate to 50% after post natal day 25 (P25). Interestingly, the majority of these mice showed severe ataxia and dystonia (Zinnanti et al. 2009).

1.8 Effects of elevated BCAA levels on the nervous

How exactly the elevated BCAA levels lead to the neurodegeneration and abnormal behavior and seizures is not yet completely understood. Most likely it is a combination of synergistic effects of several inhibiting and damaging cascades with

systemic effects throughout the embryo (Kevin A. Strauss and Morton 2003). One aspect is a metabolic imbalance of the neuronal environment in the brain. In the brain of calves, rodents and human patients showing abnormal levels of BCAAs a reduction of neurotransmitters such as GABA , glutamate and aspartate were significantly reduced (Dodd et al. 1992; Kevin A. Strauss and Morton 2003; Funchal et al. 2004; Zinnanti et al. 2009). This is thought to cause extracellular hypertonicity leading to edemas, a reduction of larger amino acids in the brain due to competition at the LAT1 mediated at the cerebral barrier and active transport of glutamine out of the brain (Kevin A. Strauss and Morton 2003).

1.9 Significance

Through identification and functional characterization of the *que* mutant I analyzed a gene that is essential for normal locomotion and potentially for development and/or early maintenance of neuronal networks. *que* mutants reveal a novel gene involved in network formation or maintenance and might contribute to the understanding of neurological diseases due to the history of useful contributions to the understanding of such disorders by previously identified behavioral zebrafish mutants. In addition, MSUD has a significant impact on the quality of life of patients including their mental performances. A vertebrate model capable of screening through small compound libraries would be a very useful tool to find new therapeutic strategies.

Accordion mutants	gene	description	human disorder
<i>accordion</i>	Serca1	calcium pump (muscle)	Brody's disease
<i>ziehharmonika</i>	AchE	acetylcholinesterase (muscle)	congenital myasthenic syndrome
<i>bandoneon</i>	Glr2	Glycine receptor (β subunit)	Hyperekplexia
<i>diwanka</i>	LH3	glycosyltransferase	connective tissue disorder (Salo et al. 2008)
<i>bajan</i>	ChAT	choline acetyltransferase	myasthenic syndrome
<i>DA5</i>	Serca1	calcium pump (muscle)	Brody's disease
<i>twister</i>	AChR α	acetylcholine receptor (muscle)	Slow channel congenital myasthenic syndrome
<i>quetschkommode</i>			?
<i>expander</i>			?
<i>squeezebox</i>			?

Table 1.1: Accordion Class Mutants

Mutants of the accordion class obtained from a mutagenesis screen (Granato et al. 1996). Shaded in red: muscle or muscle end plate associated mutations; in green: CNS associated mutations.

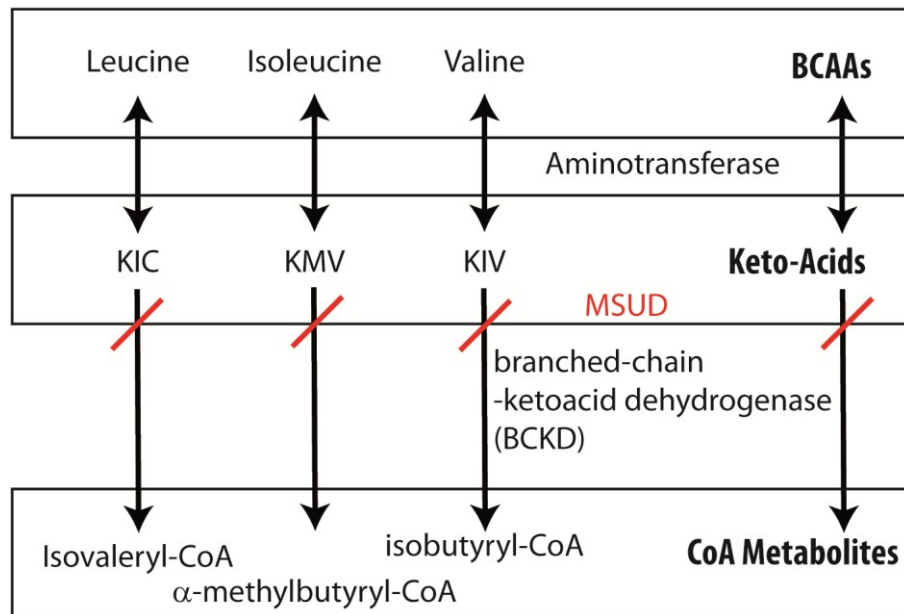


Figure 1.1: Branched Chain Amino Acid Metabolism

The first step of BCAA metabolism consists of a reversible transamination resulting in Keto acid derivatives. The second step is an oxidative decarboxylation reaction of the α -keto acids by the mitochondrial branched chain α -keto acid dehydrogenase complex (BCKD). In Maple Syrup Urine Disease activity of the BCKD is reduced or absent resulting in accumulation of BCAAs and keto acids.

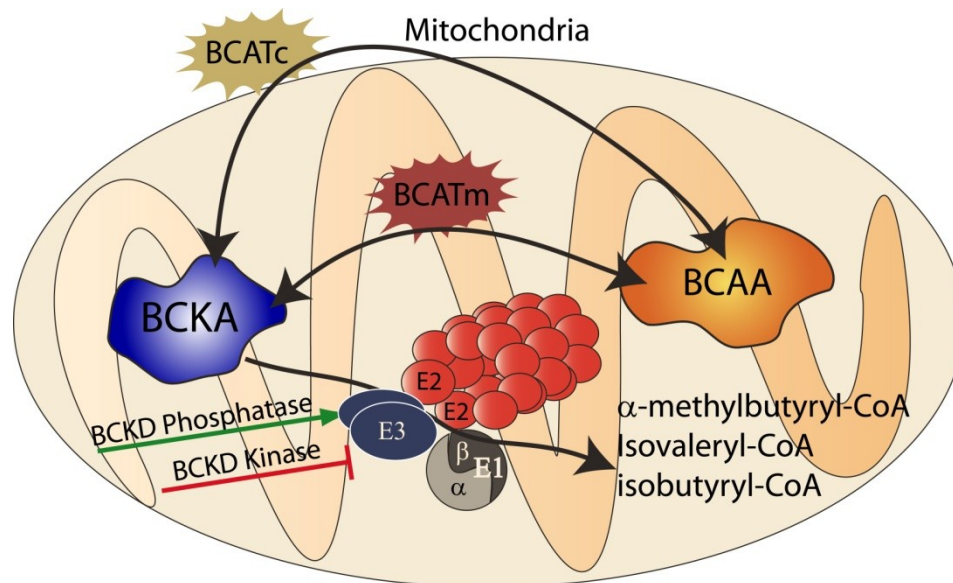


Figure 1.2: Model for regulation of Branched Chain Amino Acids in mitochondria

Multiple enzymes form the BCKD complex. Branched chain amino acid aminotransferases (BCATs) both inside and outside of the mitochondria reversibly convert branched chain amino acids (BCAAs) into their keto acid form (BCKAs). The E2 subunit functions as transacylase and forms a cubic core as a homo-24-mer. It is surrounded by 12 E1 heteromers consisting of α 2 and β 2 subunits. In addition the E2 core has six E3 homodimers attached to it which function as dehydrogenases. Its activity is regulated by regulation of its phosphorylation by the BCKD kinase and phosphatase.

CHAPTER 2

BEHAVIORAL AND ELECTROPHYSIOLOGICAL CHARACTERIZATION OF THE *QUE* MUTANT

The following section was modified from (Friedrich et al. 2012)

2.1 Abstract

A common symptom of many neurological diseases is impaired locomotor behavior. The neuronal networks required for proper locomotion are established during early development but despite recent identification of neurons involved in these networks it is still largely unknown what factors are required for proper development and function of these networks (Warp et al. 2012).

Zebrafish are an excellent model system to study these networks due to their rapid external development and a series of distinct locomotor behaviors during embryonic development. A powerful tool available in that system is a panel of motility mutants that can be used to identify novel genes and factors required for neuronal network formation and maintenance (Granato et al. 1996). From this panel I obtained the motility mutant *quetschkommode* (*que*). To assess whether its inability to swim is CNS or muscle derived I analyzed its behavior in detail and compared it to known muscle and CNS defect mutants but no distinguishable trend emerged. Since structural effects could also account for the observed phenotype I visualized critical structural components such as sensory neurons, motor neurons and muscle fibers but found no gross anomalies in the *que* mutant. To better distinguish between the possibilities of *que* mutants harboring a CNS or muscle defect, simultaneous contra-lateral peripheral nerve recordings were performed

showing a significant increase of contra-lateral overlap of CNS output indicating abnormal CNS output in the mutant.

2.2 Introduction

Zebrafish display a series of well defined locomotor behaviors throughout early development starting with spontaneous movements at 17 hpf progressing through touch evoked tail coiling and resulting in burst swimming after 27 hpf (Saint-Amant and Drapeau 1998; Buss and Drapeau 2001). This series of behaviors is thought to reflect a dynamic development and remodeling of neuronal networks in the brain and spinal cord. Despite advancements in knowledge about these neuronal networks, their components and connectivity, their formation and functional requirements during development are largely still unknown.

The *que* mutant was generated in a mutagenesis screen in 1996 (Granato et al. 1996). While wild-type larvae respond to touch with a high amplitude body-bend with the tip of the tail touching the head (C-bend) followed by alternating body bends at 4 dpf (Eaton et al. 1977; Zottoli and Faber 2000), *que* mutants are paralyzed and contract rostrocaudally. This compression resembles the contraction of the musical instrument accordion which led to the name of the accordion class. Besides the initial classification its phenotype has not been characterized in detail. From previous studies it was found, that the observed rostrocaudal compression observed in accordion class mutants can be caused by CNS defects (Hirata et al. 2005) or anomalies in muscle structure or relaxation (Downes and Granato 2004; Gleason et al. 2004; Hirata et al. 2004; Lefebvre et al. 2004; M. Wang, Wen, and Brehm 2008; Olson, Sgourdou, and Downes 2010). Independent of

the mechanism leading to the observed accordion phenotype most mutants have been associated with human diseases and have greatly contributed to their understanding. To determine whether *que* mutants harbor a CNS or muscle defect is crucial for its usefulness in studying neuronal network formation and maintenance.

For this purpose I used a quantitative behavioral analysis approach to analyze the *que* mutant phenotype in detail. I compared the *que* mutant phenotype as well as structural components of the circuitry and the muscle to known muscle and CNS defect mutants. Finally, peripheral nerve recordings were used to analyze CNS output.

2.3 Materials and methods

2.3.1 Behavioral analysis

To characterize swimming behavior at 4 dpf, at the onset of the *que* mutant behavior, light touch stimuli were applied to the head of larvae using a 1 mm insect pin. The response was recorded using a high-speed video camera (Fastec Imaging, San Diego, CA), recording 500–1000 frames per second, mounted to a 35 mm lens (Nikon, Melville, NY). The head-to-tail angle for each frame was measured using automated software developed in the Downes laboratory by Kelly Anne McKeown and Sandy Whittlesey (McKeown et al. 2012). In brief, pixel density analysis was used to identify three landmarks along the larval body: the tip of the nose, the border between the yolk ball and yolk extension, and the tip of the tail. These three points form an angle for each frame which was plotted over time using Microsoft Excel.

2.3.2 Antibody staining

Whole mount immunostaining was performed using standard protocols [similar to (Downes and Granato 2004)]. The primary antibodies were mouse anti F59 (1:10, Frank Stockdale; Stanford University, Stanford, CA) labeling fast muscle fibers, mouse anti acetylated tubulin (1:400; Sigma, St. Louis, MO) staining sensory neurons and anti SV2 (1:100, Kathleen Buckley, Stanford University, Stanford, CA) labeling synaptic vesicles of motor neurons. Secondary antibody was Alexa Fluor 594 goat anti Mouse (1:1000 dilution, A11005, Molecular Probes, Sigma, St. Louis, MO). Images were acquired using a confocal microscope (Nikon, Melville, NY). Z-stack picture series were generated and overlaid using the EZ Viewer program (Nikon, Melville, NY) and Adobe Photoshop (San Jose, CA, USA). Figure 2.2 B4 was modified from (Downes and Granato 2004).

2.3.3 Electrophysiology

Zebrafish larvae at 4 dpf were anesthetized with 0.02% Tricaine-S (Western Chemical) in extracellular recording solution (Legendre and Korn 1994; Drapeau et al. 1999; Masino and Fetcho 2005) and paralyzed with 0.1% (w/v) α -bungarotoxin (Sigma), which significantly reduced or abolished postsynaptic muscle activity based on patch recordings from muscle fibers (Masino and Fetcho 2005). The extracellular solution was superfused continuously at 22-26°C. Larvae were pinned in a dorsoventral position to a Sylgard-lined glass-bottom Petri dish and the skin was removed. Extracellular suction electrode recording techniques were used to monitor the activity of peripheral nerves during fictive behavior (Masino and Fetcho 2005). Activity occurred spontaneously but was also initiated by gently applying a touch stimulus to the head with a tungsten pin

controlled and positioned by a manual micromanipulator (MX130, Siskiyou, Grants Pass, OR). The tip of the extracellular suction electrode (~15 μm tip diameter) was positioned at the dorsoventral midline of a myotomal cleft where the skin had been removed. All extracellular recordings were restricted to between body segments 7 and 15. A MultiClamp 700B (Molecular Devices, Sunnyvale, CA) amplifier was used to monitor extracellular voltage in current-clamp mode at a gain of 1000 ($R_f=50\text{ M}\Omega$) with the low- and high-frequency cut-off at 100 and 4000 Hz, respectively. Recordings were sampled at 10 kHz. Extracellular recordings were digitized using a digitizing board (DigiData series 1440A, Molecular Devices, Sunnyvale, CA) acquired using pClamp 10 software and rectified offline.

2.4 Results and discussion

2.4.1 *que* mutants exhibit abnormal rostrocaudal compressions in response to touch

A single allele of *que* (ti274) was identified from a previously performed mutagenesis screen (Granato et al. 1996; Zottoli and Faber 2000). The mutation is recessive, and homozygous mutants first demonstrate abnormal rostrocaudal compressions at around 72 hpf (data not shown). The abnormal behavior becomes more robust by 96 hpf. At this time point, high-speed video analysis shows that wild-type larvae respond to touch by first performing a large amplitude body bend, defined here as greater than 110° , followed by lower-amplitude body undulations to swim away (Figure 2.1A). By contrast, *que* mutants do not perform the initial C-bend or lower-amplitude body undulations, and instead demonstrate rostrocaudal shortening (Figure 2.1B). Other mutants have been shown to demonstrate this accordion behavior due to defects in either

CNS function, such as *bandoneon* (*beo*, Table 2.1) (Hirata et al. 2005), or muscle relaxation, such as *accordion* (*acc*, Table 2.1) (Gleason et al. 2004; Hirata et al. 2004; Hirata et al. 2005; Olson, Sgourdou, and Downes 2010). I used kinematic analysis to analyze the swimming behavior of *que* mutants and compare it to the CNS defect mutant *beo* and the muscle defect mutant *acc* to determine whether I could distinguish defects in CNS function from defects in muscle relaxation. No clear trend emerged; however, *que* mutants consistently show the most dramatic disruption of swimming behavior compared to *acc* or *beo* mutants. Although *acc* and *beo* mutants demonstrate abnormal swimming behavior, C-bends are often observed (Figure 2.1C-E). By contrast, *que* mutants very rarely execute large-amplitude body bends (Figure 2.1F). *que* mutants continue to perform accordion behavior 5-6 days post-fertilization (dpf). They fail to inflate the swim bladder, which would enable them to feed, and eventually die around 7 dpf.

2.4.2 *que* mutants do not exhibit gross muscle or nerve structure defects

It has been shown that the accordion phenotype can result from CNS defects as well as muscle defects (Downes and Granato 2004; Hirata et al. 2005) or might result from secondary structural defects in sensory and/or motor neurons. To visualize potential structural defects in these tissues antibody staining for fast muscle fibers (Figure 2.2B), developing sensory neurons (Figure 2.2C) and motor neurons (Figure 2.2D) was performed. The results for *que* were compared to wild-type and *beo* mutants as well as to *ziehharmonika* (*zim*) (Downes and Granato 2004), a known muscle mutant with structural defects in muscle development. Defects observed in muscle fiber patterning observed in the *zim* mutant (Figure 2.2 B4) were not observed in *que* mutants (Figure 2.2 B3). No severe structural abnormalities were observed in sensory neurons (Figure 2.2C3) or motor

neurons (Figure 2.2 D3). Although smaller defects in synapse distribution and interneurons cannot be ruled out at this level of analysis, the absence of gross structural defects is consistent with the hypothesis that the mutation does not affect behavior through altering muscle structure.

2.4.3 *que* mutants demonstrate abnormal CNS motor output

To better examine whether *que* mutants harbor a defect in CNS function as opposed to a defect in muscle relaxation, we analyzed fictive locomotor output from the spinal cord by performing extracellular peripheral nerve recordings on motor neurons of paralyzed larvae. This analysis was performed in collaboration with Aaron Lambert and Mark Masino at the University of Minnesota. Zebrafish larvae demonstrate bouts of motor output in response to touch (Figure 2.3 A,B). These bouts are composed of tightly coordinated bursts that alternate rapidly between the left and right sides and orchestrate the axial muscle contractions that constitute swimming. In wild-type larvae, we observed rapid alternations in locomotor output between the left and right sides with little overlap in bursting activity ($6.5 \pm 6\%$, $n=5$; Figure 2.3C), as described previously (Masino and Fetcho 2005). In *que* mutants, although the coordination of left-right locomotor activity was similar to wild-type siblings (compare Figure 2.3C, D), the amount of overlap between left-right bursting activity was significantly higher ($19.1 \pm 11.3\%$, $n=7$; $t = -2.3$, $p < 0.05$). This increase in activity overlap is consistent with the simultaneous left-right muscle contractions performed by *que* mutants. These data do not rule out the possibility that *que* mutants contain a defect in muscle relaxation; however they indicate that abnormal motor output from the CNS at least contributes to this mutant's behavior. To further characterize potential differences in locomotor output between wild-type and

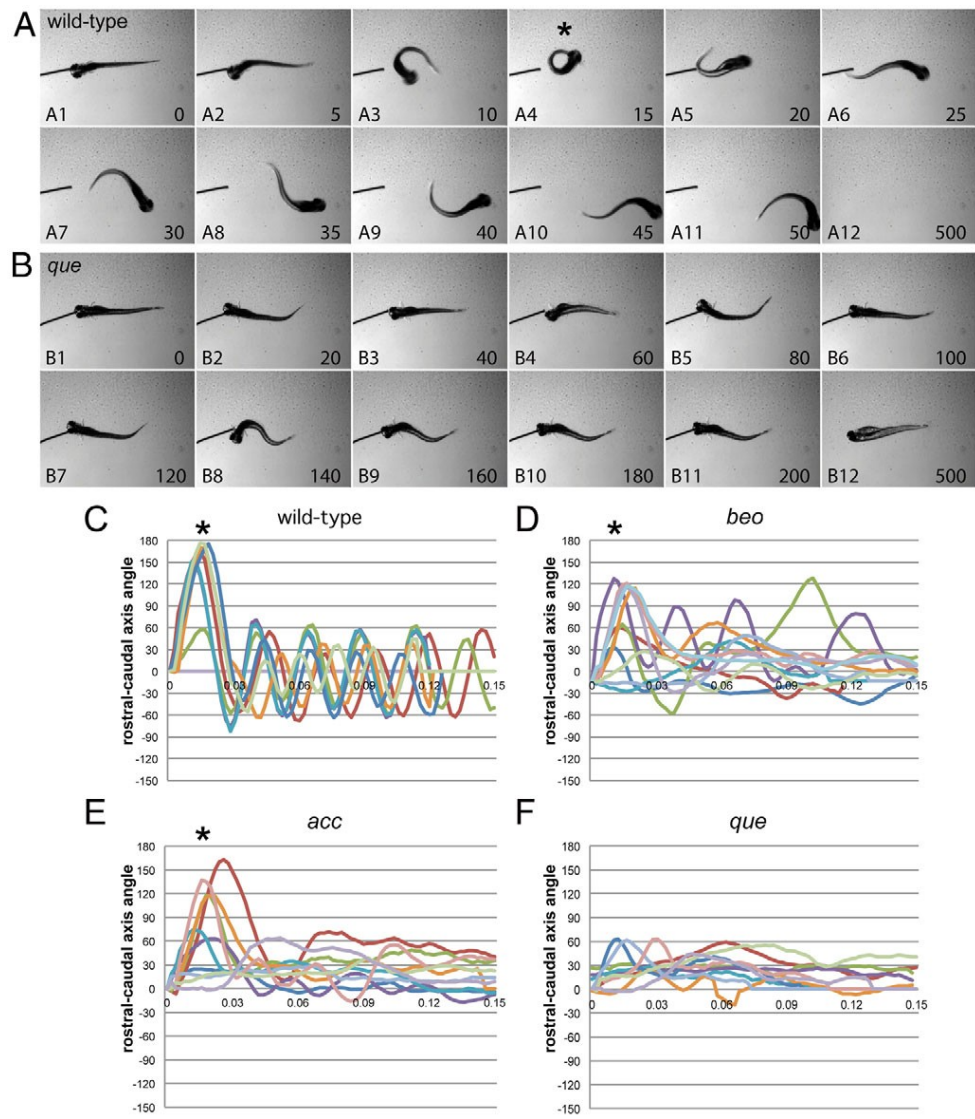
que mutant siblings, we examined a range of bout and burst properties related to rhythmic locomotor activity during fictive swimming (Masino and Fetcho 2005). Though most of these properties were not significantly different between wild-type and mutant larvae, *que* mutants generated a significantly greater number of bouts following the touch stimulus applied to the head than did wild-type larvae [11.6 +/- 6.2 bouts and 1.9 +/- 0.9 bouts, respectively ($t = 3.5$, $p < 0.01$, $n = 5$)]. These results suggest that there are subtle, yet significant, changes in the locomotor circuit that underlie swimming in *que* mutant larvae that participate in generating the mutant behavioral phenotype.

2.4.4 Significance

I characterized the behavior of *que* mutants in detail. I showed that *que* mutants begin to show abnormal behavior around 4 dpf in our mixed genetic background. They exhibit a reduction of both C-bend amplitude and alternate body bends afterwards and quickly become paralyzed. I visualized structural components of the escape response circuitry and found no obvious structural effects consistent with the hypothesis that the behavior observed is not based on structural abnormalities obtained during development. We analyzed the CNS output and found significant overlap of left-right motor output suggesting that the mutation directly or indirectly affects the escape circuitry at or upstream of motor neurons.

Figure 2.1: *que* mutants exhibit abnormal swimming behavior at 96 hpf

(A,B) Selected frames from high-speed video recordings are shown with times indicated in milliseconds. (A) A wild-type larva demonstrates a normal C-bend (A4, asterisk) in response to a touch stimulus, followed by smaller-amplitude body undulations to clear the field (A5-A12). (B) A *que* mutant demonstrates abnormal rostrocaudal shortening and it fails to escape. (C-F) Kinematic traces are shown, with zero degrees indicating a straight body and positive and negative angles representing body bends in opposite directions. Time is shown in seconds. Ten representative traces are shown for each phenotype. (C) Wild-type embryos typically perform a C-bend (defined here as greater than 110°; asterisks) followed by smaller-amplitude body undulations. (D) *bandoneon* (*beo*) mutants, which contain a CNS defect and demonstrate behavior similar to *que*, sometimes perform a C-bend followed by abnormal body bends. (E) *accordion* (*acc*) mutants, which contain a muscle relaxation defect and also demonstrate behavior similar to *que*, sometimes perform a C-bend but fail to perform smaller-amplitude body bends. (F) *que* mutants rarely perform a C-bend and demonstrate few smaller amplitude body undulations.



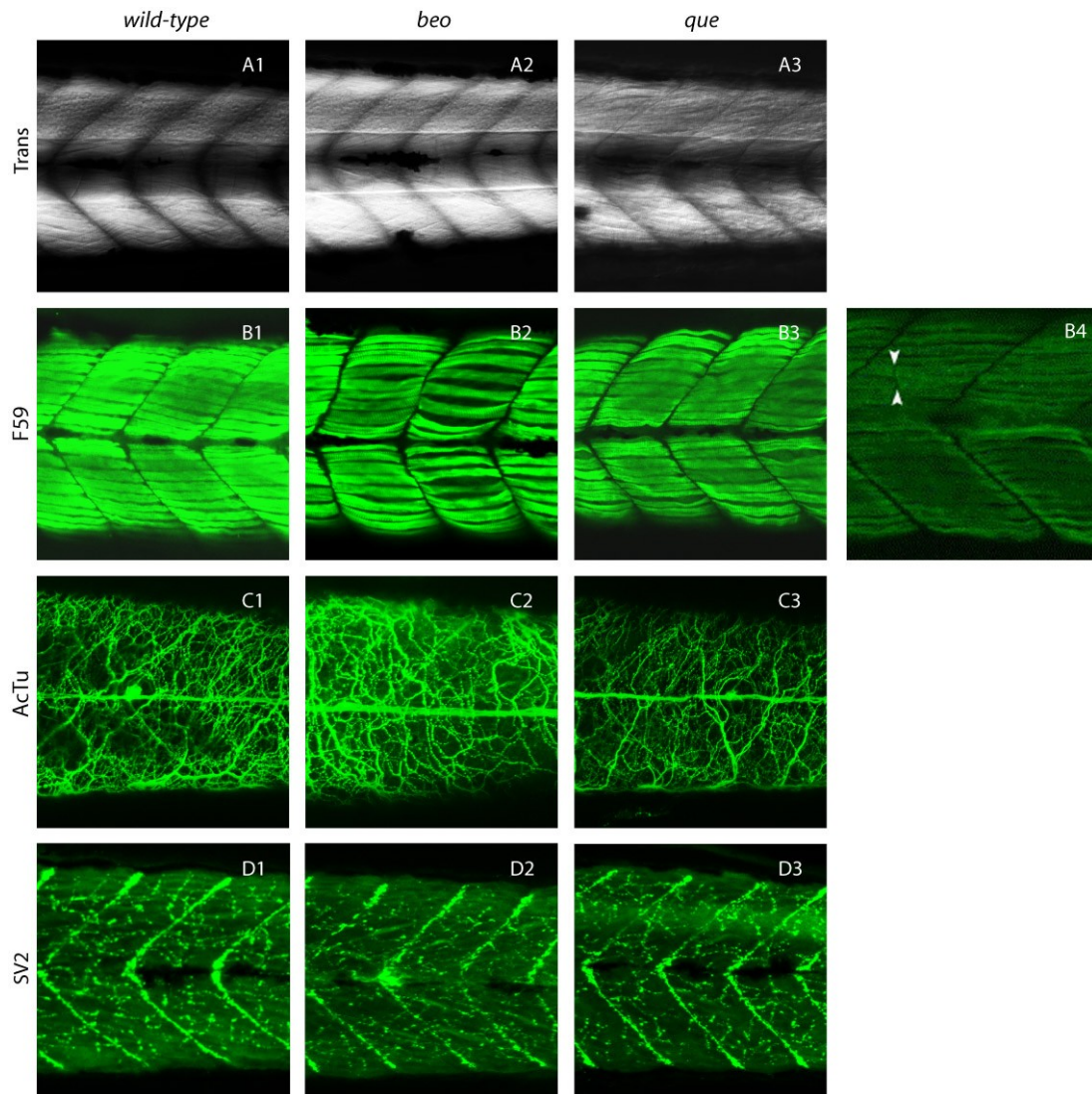


Figure 2.2: *que* mutants do not exhibit gross nerve or muscle structure defects

In each panel, lateral views are shown, with dorsal up and rostral to the left. Embryos of *que* and wild-type embryos at 96 hpf were stained with antibodies against F59 (fast muscle myosin), acetylated tubulin (developing sensory neurons) and SV2 (motor neurons). The muscle fiber alignment is normal in both mutants (B1-B3). Both, sensory (C1-C3) and motor neuron projections (D1-D3) do not differ in location and distribution in either mutant compared to wild-type (A1-D1). Structural defects observed in the muscle mutant *zim* (B4) (Downes and Granato 2004) were neither observed in *que* nor *beo* mutants.

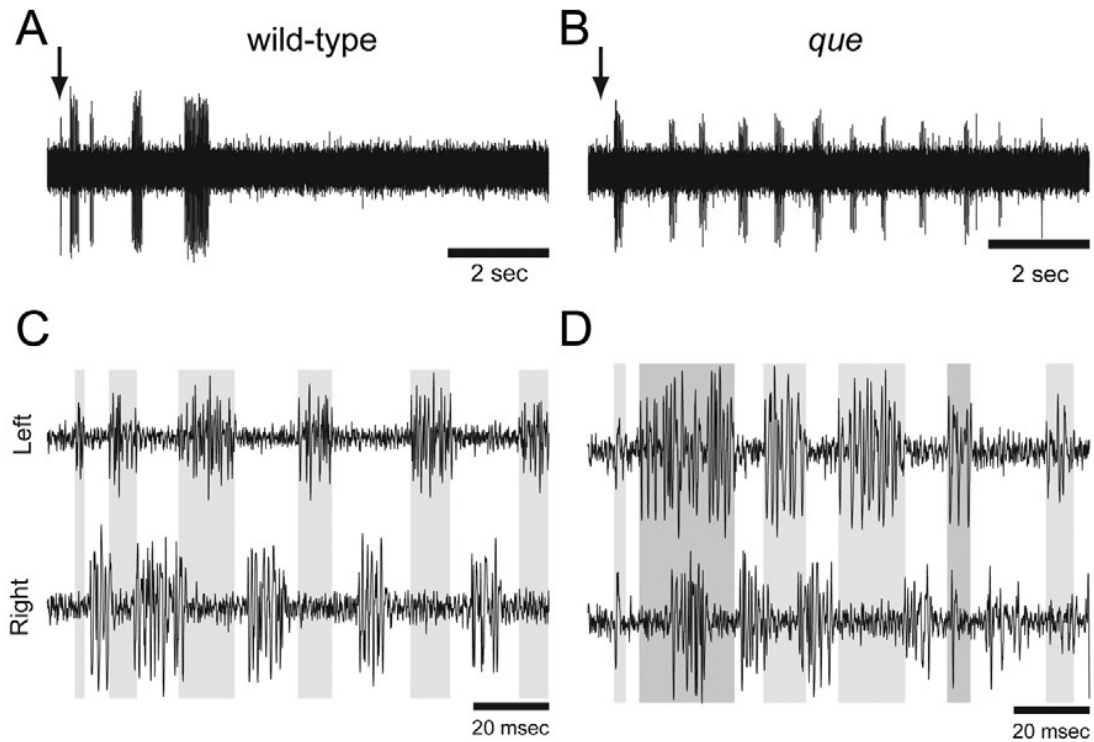


Figure 2.3: The spinal locomotor output is altered in *que* mutants

(A,B) Representative single extracellular peripheral nerve recordings from (A) wild-type and (B) a *que* mutant. *que* mutants produce a greater number of bouts following a gentle tap to the head (arrow) than do wild-type. (C,D) Representative paired (left-right) extracellular peripheral nerve recordings in which (C) wild-type fish demonstrate tightly coordinated bursting activity with little overlap. By contrast, (D) *que* mutants generate greater bursting overlap. Gray bars denote burst activity in the top trace and extend to the bottom trace for ease of comparison.

bout and burst properties	Wild-type	<i>que</i> mutants
No. of bouts	1.9±0.9	8.6±7.3*
Bout duration (msec)	329.1±60.4	285.2±148.8
No. of bursts per bout	9.5±1.9	9.7±3.6
Burst duration (msec)	13.3±2.8	12.4±1.7
Burst duty cycle (%)	30.9±11.8	39.6±6.8
Burst frequency (Hz)	31.6±4.6	37.6±9.3
Mean contra-lateral phase (%)	49.6±1.2	50.4±7.7
Bursting overlap (%)	6.5±6.0	19.1±11.3**

Table 2.1: Comparison of bout and burst properties related to fictive locomotor activity in wild-type and *que* mutants

All values presented as mean ± s.d. Significant differences are indicated by *P<0.05 or **P<0.01.

CHAPTER 3

MOLECULAR IDENTIFICATION OF THE *QUE* LOCUS

3.1 Abstract

In the previous study the results suggested that the abnormal locomotor phenotype observed in *que* mutants is at least partially due to abnormal CNS output (Chapter 2). Therefore the mutated gene in the *que* larvae promises to be essential for locomotor network development and/or function. I mapped the *que* gene to 0.36cM on chromosome 22 and found a splice site mutation in the splice donor site of exon 6 of dihydrolipoamide branched chain transacylase E2 (*dbt*). This enzyme is one of the key enzymes in branched chain amino acid metabolism and can cause Maple Syrup Urine Disease (MSUD) when DBT is mutated in humans. Embryos injected with an anti-*dbt* morpholino showed reduction of *dbt* protein expression and similar reduction of C-bend and alternating body bends as *que* mutants. Taken together these results suggest *dbt* is the gene mutated in *que* mutants.

3.2 Introduction

The aim of this study is to characterize the zebrafish mutant *que* and use it as a tool to study neuronal network formation and maintenance. In the previous study (chapter 2) abnormal CNS output was observed in addition to disrupted locomotor behavior consistent with the hypothesis that the observed disrupted ability to swim is at least partially based on impaired neuronal networks. Having thus established that abnormal CNS output is most like contributing to the abnormal locomotor behavior, I pursued a positional cloning approach to determine the mutated gene in *que* mutants, which is

required to better understand the mechanism behind the seizure like behavior of *que* mutants and to identify potential corresponding genetic disorders in humans.

3.3 Methods

3.3.1 Chromosomal mapping and sequence analysis

Crosses between fish heterozygous for the *que* allele (carriers) and WIK fish were used to generate a three-generation map cross panel. F2 *que* mutant embryos and wild-type siblings were collected, sorted based upon the 96 hpf phenotype and stored in methanol at -20°C . DNA was extracted from more than 833 mutant larvae, and SSLP markers and SNP markers were obtained and generated against genes to refine the mapping interval. Exons and intron-exon boundaries of candidate genes were sequenced (Genewiz, South Plainfield, NY) from wild-type, *que* siblings and homozygous mutants.

3.3.2 Morpholino analysis

Wild-type zebrafish embryos were pressure injected at the one- to four-cell stage with 12 ng of morpholino designed to block translation of *dbt* or the standard control morpholino (Gene Tools, Phinomath, OR). This amount of morpholino was selected based upon dose-response experiments in which higher doses were found to generate morphological defects and/or lethality. The sequence of the translation-blocking morpholino was 5'-CGCACAGTAAATGACCGCCGCCATCT-3'. Underlined residues indicate the start codon. The control morpholino sequence was

5'-CCTCTTACCTCAGTTACAATTTATA-3'. The embryos were raised at 28.5°C, and locomotive behavior was examined across development. Kinematic analysis, as described above, was performed at 96 hpf.

3.4 Results and discussion

3.4.1 Chromosomal mapping and sequence analysis

To determine the molecular identity of the *que* gene, I used a positional cloning strategy. Using a three-generation map cross panel, I screened pools of genomic DNA from wild-type siblings and homozygous mutants with a panel of simple-sequence length polymorphism (SSLP) markers. *que* mapped to chromosome 22, which confirmed previous low-resolution mapping results (Geisler et al. 2007). I then used DNA extracted from single embryos and single nucleotide polymorphism markers to refine the map position to a 0.36cM interval between the markers ENSDART109865 and wu:f63d09 (Figure 3.2A). Extensive genome database analysis and sequencing of nearby candidate genes led me to dihydrolipoamide branched chain transacylase E2 (*dbt*), a subunit of the BCKD complex, which is required for BCAA metabolism. Zebrafish *dbt* is a predicted 493 amino acids in length, and it is ~78.2% identical to the human protein (Figure 3.1). Mutations in the human DBT gene are known to cause MSUD, which can result in severe dystonia and death if not treated. Given that *que* mutants demonstrate abnormal behavior and nervous system function consistent with the severe dystonia observed in humans, I sequenced the *dbt* gene. Sequence analysis of the *dbt* gene from *que* homozygotes revealed a single nucleotide substitution compared to wild-type in the splice donor site of exon 6. The guanine of the intron side of this splice site is changed to an adenine (Figure

3.2B). To determine whether this change affects the splicing of intron 6 as would be predicted, I performed RT-PCR using one primer in exon 6 and one primer in exon 7 (Figure 3.2C). I found that RNA extracts from wild-type larvae were spliced according to prediction, however RNA extracts from homozygous mutants revealed a larger transcript that contained the entire 86 base pairs of intron 6, indicating it was spliced incorrectly (data not shown). This intron alters the sequence downstream of Lysine268 and contains four stop codons, which would prematurely truncate the *dbt* protein by 224 amino acids. *dbt* contains an acetyl transferase domain, essential for its function (Chuang, D. T., Wynn, R. M. and Shih, V. E. 2008), which would be largely absent from the *que* mutant protein. Interestingly, in humans, a mutation that prematurely truncates the DBT protein at the orthologous position (Lysine257) was reported in an individual with the most severe or ‘classic’ form of MSUD (Herring et al. 1992; Chuang, D. T., Wynn, R. M. and Shih, V. E. 2008). These data indicate that the *que* mutation is a loss-of-function allele that diminishes or abolishes BCKD complex function.

3.4.2 Confirmation through phenocopying

To further confirm the molecular identity of *que*, I injected wild-type embryos with either a standard control morpholino or a morpholino designed to block translation of *dbt*. Embryos were injected at the 1-4 cell stage and monitored over the course of development. Embryos injected with the standard control morpholino exhibited mostly normal behavior throughout the course of development (97.2% of surviving larvae, n=107; Figure 3.2D). Notably, 37.5% (n=144) of surviving larvae injected with the morpholino designed to target *dbt* demonstrated clear rostrocaudal compressions and fewer large amplitude body bends at 96 hpf, similar to *que* mutants (Figure 3.2E). In

addition, I noticed a strong decrease of *dbt* protein in the mutant (Figure 3.3). It is important to note that morpholinos are known to lose effectiveness ~4-5 dpf due to turnover, which likely explains why not all embryos injected with the *dbt* morpholino demonstrated the robust accordion behavior exhibited by *que* mutants (Bill et al. 2009). I also attempted to perform rescue experiments in mutant embryos by injecting mRNA encoding *dbt* at the 1-4 cell stage and analyzing motility behavior at 4 dpf. I did not observe rescue (data not shown), however mRNA is known to lose effectiveness ~2 dpf due to turnover. The *que* behavioral phenotype is not apparent until 3-4 dpf, which indicates that *dbt* is required at this stage of development and precludes mRNA rescue. Regardless, the mapping data, nature of the *que* mutation, aberrant mRNA splicing observed in mutants, the morpholino phenocopy and the reduced levels of *dbt* protein in *que* mutants all argue that the *que* gene encodes *dbt*.

3.5 Significance

I mapped the mutation in *que* mutants to chromosome 22 and found a mutation in *dbt*, a key enzyme in the branched chain amino acid metabolism. A homologous truncation of *dbt* has been found in human patients suffering from MSUD (Chuang, D. T., Wynn, R. M. and Shih, V. E. 2008). This suggests that the *que* mutant harbors a mutation similar to those found in MSUD patients leading to the observed seizure-like phenotype.

```

Human DBT 1 MAAVRMLRTWSRNAGKLICVRYFQTCGNVHVLKPNYVCFPGYP---SFKYSHPHFLKTTAALRGQVVQFKLSDIG
          MAAV +R      +L+ R + C +   K   C   P   S   H + T+      +VQFKLSDIG
Zfish DBT 1 MAAVITVRAPFVFMRRLV SARLHRNCCS----KLPAACLVL RPHSYSLVAGRQHRFYHTSYVAARPIVQFKLSDIG

74 EGIREVTVKEWYVKEGDTVSQFDSICEVQSDKASVTITSRYDGVIKKLYNLDIAYVGKPLVDIETEA--LKDSEEDVVETPAV
   EGI EVTVKEWYVKEGD VSQFDSICEVQSDKASVTITSRYDGV I+KLYY++D IA VGKPLVDIET+   + +EDVVETPAV
73 EGIMEVTVKEWYVKEGDKVSQFDSICEVQSDKASVTITSRYDGVIRKLYYDVDSIALVGKPLVDIETDGGQAESPQEDVVETPAV

157 SHDETHQEIKGRKTLATPAVRRLAMENNIKLVSEVVGSGKDGRILKEDIILNYLEKQTGAILPPSPKVEIMPPPP-----K
    S +EH+ QEIKG KT ATPAVRRLAMENNIKLVSEVVG+GKDGRILKEDIILN++ KQTGAILPP+P EI P PP           K
158 SQEEHSPQEIKGHKTQATPAVRRLAMENNIKLVSEVVGTKDGRILKEDIILNFIKQTGAILPPAPFQEI RPPAAAAPLTPSAK

232 PKDMTVPIVSKPPVFTGKDKTEPIKGFQKAMVKTMSAALKIPHFGYCDIDLTELVKLREELKPIAFARGIKLSFMPFFLKAAS
    +VPI V   PVFTGKD TEPIKGFQKAMVKTMSAALKIPHFGY DE+DL++LV+LR ELK + +RG+KLS+MPFF+KAAS
243 ATPSPVPIVPIPKPVFTGKDHTEPIKGFQKAMVKTMSAALKIPHFGYKDEV DLSQLVRLRSELKGLTESRGVKLSYMPFFIKAAS

317 LGLLQFPILNASVDENCQNITYKASHNIGIAMDTEQGLIVPNVKNVQICSFIDIA TELNRLQKLG SVGQLSTTDLTG GTFTLSNI
    L LL FPILN+S+DENC +ITYKA+HNIG+AMDT QGL+VENVKN+Q+ S+F+IA ELNRLQ LG+ GQL T+DLTG GTFTLSNI
328 LALLHFPILNSSLDENCTSI TYKAAHNIGLAMDTSQGLLVPNVKNIQMLSVFEI AVELNRLQILGASGQLGTS DLTG GTFTLSNI

402 GSIGGTFKPVIMPPEVAIGALGSIKAI PRFNQKGEVYKAQIMNVSW SADHRVIDGATMSRFSNLWKSYLENPAFM LLDLK 482
    GSIGGT+AKPVI+PPEVAIGALG I+ +PRFN K EV KA IMNVSW SADHR+IDGATM RFSNLW+SYLENPA M+LDLK
413 GSIGGTYAKPVILPPEVAIGALGKIQVLRFRFNH KDEVVKAHIMNVSW SADHRIIDGATMCRFSNLWRSYLENPA SMVLDLK 493

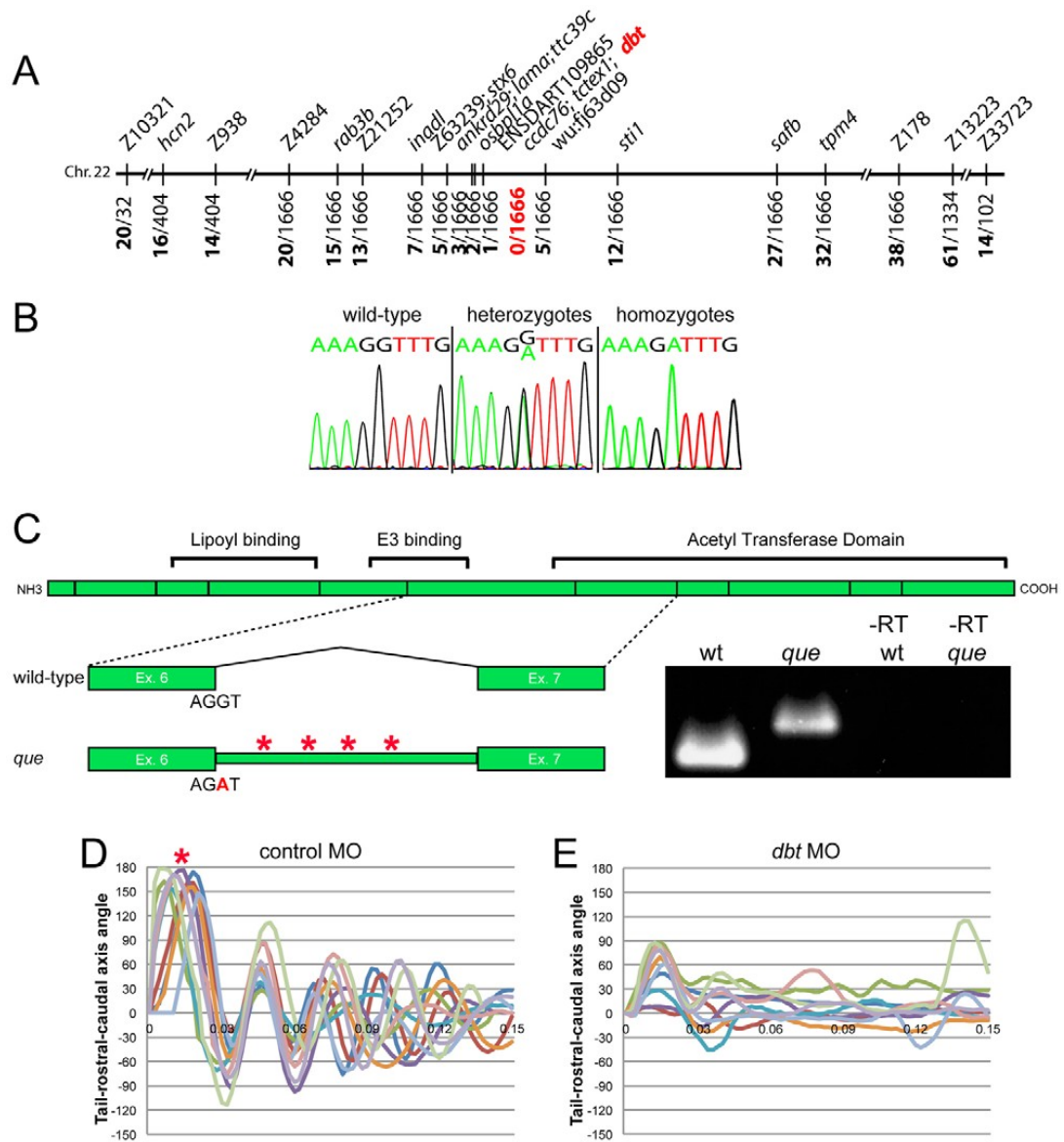
```

Figure 3.1: Protein sequence alignment of human and zebrafish *dbt*

Needleman-Wunsch alignment. Identity: 68%. Similarity: 78%. Gaps: 5%. A plus indicates different amino acids with similar properties.

Figure 3.2: The *que* gene encodes dihydrolipoamide branched-chain transacylase E2 (*dbt*), a subunit of the BCKD complex

(A) *que* maps to a 0.36 cM interval on chromosome 22. Molecular markers are shown at the top and the number of recombinants out of the number of meiotic events is shown at bottom. *dbt* was positioned within the zero recombinant interval. (B) Chromatogram sequence traces of *dbt* from wild-type, hetero and homozygous mutant larvae. The nucleotide substitution at the exon-intron boundary (G to A) can be observed in hetero- and homozygotes. (C) A schematic of the *dbt* protein is shown with the boundaries between exons indicated as vertical lines. Protein domains, including the acetyl transferase domain, are also shown. Below, the wild-type splice pattern is illustrated, with protein-coding exon 6, the sequence at the splice site, the intervening intron, and protein coding exon 7 depicted. The *que* mutant splicing pattern is also illustrated, including the nucleotide substitution, which results in a failure to remove the intron. The intron contains four stop codons (asterisks). RT-PCR results using mRNA from wild-type, *que* mutants and –RT controls are also shown using primers targeted towards exon 6 and exon 7. A larger DNA product, containing intron sequence, can be observed using mRNA isolated from *que* mutants. (D,E) Ten kinematic traces are shown for embryos injected with (D) the control morpholino or (E) a *dbt* translation-blocking morpholino. Embryos injected with the control morpholino perform C-bends (asterisk) and normal swimming behavior. *dbt* morphant embryos demonstrate abnormal swimming behavior and few large amplitude body bends, similar to *que* mutants.



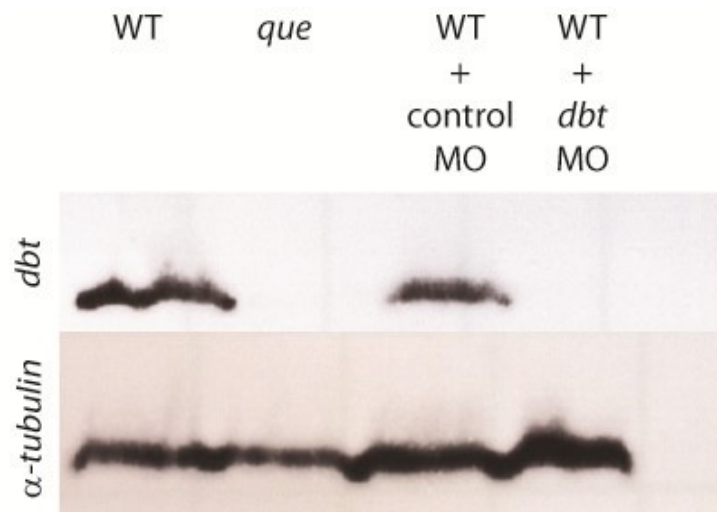


Figure 3.3: *dbt* morpholino decreases *dbt* protein levels

Western blot analysis confirmed decreased *dbt* expression in morpholino treated embryos. Top: anti-*dbt* staining. Bottom: α -tubulin as loading control.

CHAPTER 4

FUNCTIONAL CHARACTERIZATION OF THE DIHYDROLIPOAMIDE BRANCH CHAIN TRANSACYLASE E2 GENE

4.1 Abstract

To characterize *dbt* expression in zebrafish I analyzed spatial and temporal expression of *dbt* using RT-PCR and in situ hybridization. *dbt* is expressed throughout early development with maternal deposition of the transcript. Since MSUD patients display a strong increase of BCAAs as one of the key symptoms of MSUD I quantified free amino acid levels in the *que* mutant and found significantly increased levels of BCAAs as well as a decrease of neurotransmitters such as glutamate, a decrease that takes place in neuronal tissue such as the brain and spinal cord. To further validate the *que* mutant as new model of MSUD I performed a pilot drug screen showing that *que* mutant clutches perform significantly better in the presence of phenylbutyrate; a therapeutic drug currently in clinical trials. These results suggest that the zebrafish *que* mutant as a new vertebrate model to study MSUD.

4.2 Introduction

Previous studies have shown that the *que* mutant harbors a mutation in *dbt* (Chapter 3) leading to abnormal CNS output and seizure-like behavior (Chapter 2). It is not yet known when and where *dbt* is expressed during development in zebrafish. Mutations in DBT in humans lead to Maple Syrup Urine Disease which is diagnosed by elevated branched chain amino acids (Morton et al. 2002). It is unknown whether a mutation in the BCAA metabolism in zebrafish causes the same increase of BCAA.

Zebrafish larvae contain a smaller nervous system than do mammalian systems, with fewer numbers of cells. *que* mutants could therefore be a promising system to better characterize the CNS injury caused by the toxicity of elevated BCAA levels. Moreover, aquatic nature, the small size, external development and the ability to obtain large numbers of zebrafish embryos make them a useful model system for small-molecule screens (Zon and Peterson 2010). The behavioral phenotype of *que* mutants is robust and easily quantifiable; therefore, *que* mutants could be developed into a high throughput system to screen libraries of compounds to identify small molecules that improve swimming behavior. In a pilot drug screen I tested effects of three different categories of compounds: BCAAs and BCKAs for their role in the BCAA pathway as well as known and suspected beneficial drugs based on clinical trials and previous results. Compounds that improve the behavioral phenotype of *que* mutants could be candidate therapeutics for individuals with MSUD.

4.3 Methods

4.3.1 RT-PCR

RT-PCR was used to analyze mRNA splicing in mutants as well as examine expression during development. Primers designed against *dbt* gene exon 6 (5' ATCAAATAAGCGAAGTTGTCGG-3') and exon 7 (5'-GCGCAACCGGACCAAC-3') were used to amplify cDNA from wild-type and homozygous *que* mutant larvae. The primers used to amplify β -actin were 5'-CACACCGTGCCCATCTATGA-3' and 5' AGGATCTTCATCAGGTAGTCTGTCTCAG-3'. The RNAs were reverse transcribed using the Omniscript Kit (Qiagen, Venlo, Netherlands). The *dbt* PCR products were

sequenced for confirmation (Genewiz, South Plainfield, NY). RT-PCR reactions were performed multiple times to decrease the likelihood of amplification artifacts.

4.3.2 Whole-mount in situ hybridization

Antisense digoxigenin probes were generated against *dbt* using cDNA (Genbank ID BC090917) acquired from Open Biosystems (Huntsville, AL). Whole-mount, colorimetric in situ hybridization was performed using established protocols (Thisse and Thisse 2008) and examined using a compound microscope (Zeiss, Thornwood, NY) attached to a digital camera (Zeiss, Thornwood, NY). Cross sections were generated by hand sectioning in situ hybridization stained embryos with a razor blade attached to a surgical blade holder. To generate sagittal sections, in situ hybridization stained embryos were embedded in 1.5% Agar and 5% sucrose. Blocks were kept in 30% sucrose solution overnight. The next day blocks were cut into 20 μ m thick sections using a cryostat (Leica, Buffalo Grove, IL).

4.3.3 Western Blot Analysis

Western Blot analysis was performed using 4 or 5 dpf larvae lysates using 100 larvae per condition. Proteins were resolved using SDS-PAGE and transferred to a nitrocellulose membrane, blocked in PBST containing (v/w) 5% dehydrated milk and incubated in primary antibody at 4°C on a rocking platform. Primary antibodies used were Anti-DBT (1:1000; Sigma, HPA026485, St Louis, MO) and Anti- α -tubulin (1:50; 12G10 DSHB, Iowa City, IA). The transferred blot was washed, incubated in anti-rabbit-HRP (1:90000; Pierce, IL) or anti-mouse-HRP (1:30 000, Pierce, Rockford, IL) and

detected with Immun-Star (Bio Rad, Hercules, CA) or a homemade luminol based detection protocol.

4.3.4 Amino Acid Quantification

50 larvae at 96 hpf were sorted based upon the locomotor phenotype, for each amino acid quantification experiment. The larvae were flash frozen in liquid nitrogen and stored at -80°C. The samples were then homogenized and precipitated with 0.1M Lithium Citrate, 3.3% 5-sulphosalicylic acid. The samples were sonicated for 10 minutes and then centrifuged at 4,600g for 20 minutes. The supernatant was then applied to VivaSpin500 size exclusion columns (Sartorium, Germany) and centrifuged at 15,000g for 4 hours. The flow-through was stored at -80°C then sent to the University of California Davis California Genome and Proteomics Center to resolve free amino acid concentrations.

4.3.5 Immunohistochemistry

The tissue was prepared by embedding 96 hpf larvae as described for in situ hybridization. Double immunostaining was performed using standard protocols [similar to (Downes and Granato 2004)]. The primary antibodies were Rabbit anti L-Glutamate (1:100, ab9440, Abcam, Cambridge, MA) or rabbit anti DBT (1:500, HPA026485, Sigma, St. Louis, MO) and Mouse anti Acetylated Tubulin (1:200, T6793, Sigma, St. Louis, MO).

Secondary antibodies were Alexa Fluor 488 goat anti Rabbit (1:1000, A11034, Molecular Probes/Sigma, St. Louis, MO) and Alexa Fluor 594 goat anti Mouse (1:1000, A11005, Molecular Probes, Sigma, St. Louis, MO). Slides were mounted using DAPI containing Vectashield (Vector Laboratories, Burlingame, CA). Images were acquired

using a confocal microscope (Nikon, Melville, NY). The fluorescent intensity for acetylated tubulin and L-glutamate antibody staining was quantified using the EZ Viewer program (Nikon, Melville, NY) by collecting entire frames (101283mm²) or selecting a region of interest above the notochord (3060mm²) for both channels. The numbers used for quantification are the Analog to Digital Converter (ADC) values of L-glutamate normalized to acetylated tubulin.

4.3.6 Pharmacological approach

This series of experiments was performed together with Sruthi Satishchandran and Laura Stapler. To determine an effective drug concentration dechorionated wild-type larvae were incubated in a drug concentration series (range: 100nM-100mM, 5x steps, 1% DMSO, see Table 4.1) at 24 hpf for 3 days. The concentration chosen was the highest drug concentration without behavioral or developmental effect in wild-type and less than 15% mortality. Wild-type and *que* mutant clutches were incubated in either the effective concentration of a given drug or raised in E3 containing 1% DMSO. To examine swimming behavior at 96 hpf, a touch stimulus was used by means of a defined probe applying a force of not more than 32mN. To perform time-trial assays, single 96 hpf zebrafish larvae were placed at the center of a bull's eye consisting of concentric circles in 2mm intervals (Figure 4.7). The 4mm distance proved to be most accurate. The larvae were gently touched on the head and the escape response was recorded using the high-speed video camera recording at 1000 frames/second. The amount of time was measured from when the larval head crossed over the boundary of the inner circle and touched the outer circle. Individual larvae were tested once, entire clutches were assayed, and each condition was performed multiple times by two different observers. The results were

compiled into graphs using DeltaGraph (Redrock Software, Salt Lake City, UT).

Statistical analysis was performed to compare the average swim times between all conditions using the student's t-test.

4.4 Results and Discussion

4.4.1 *dbt* mRNA becomes enriched in the brain and gut organs during development

I examined the spatial and temporal expression of *dbt* in developing zebrafish. RT-PCR revealed that *dbt* mRNA was present at all time points examined from 6 hpf to 120 hpf (Figure 4.1A). In situ hybridization also confirmed early expression at the two cell stage. *dbt* was detected at the two-cell stage, indicating it is a maternally deposited mRNA (Figure 4.1B). The spatial expression of *dbt* is initially widespread through 24 hpf (Figure 4.1C,D); however, its expression pattern over the next few days of development becomes enriched in the brain and organs in the gut, such as liver and intestine (Figure 4.1E-H). These data suggest that *dbt* plays an important role in BCAA metabolism through function in these tissues. The prominent expression within the brain, in particular, suggests that *dbt* is important for CNS function.

To determine the distribution of *dbt* protein during development antibody staining was performed on cross sections of the area above the yolk extension. Due to the high protein sequence similarity (Figure 4.1) I tested an antibody against human DBT in zebrafish (Figure 4.3). In wild-type an increase of *dbt* protein expression is observed in the periphery as well as in the spinal cord (Figure 4.2C). At 96 hpf *dbt* protein localization is enriched in peripheral structures (Figure 4.2D). It can be detected in the gut as well as in the developing pronephric ducts (Figure 4.2J white and orange arrow

respectively). In the mutant *dbt* seems to be mostly absent (Figure 4.2E-H). Intriguingly, the expression pattern of *dbt*, with progressive enrichment in the brain and gut organs over the course of development, is reminiscent of another mitochondrial protein that is important for CNS function, Opa3 (Pei et al. 2010).

4.4.2 *que* mutants harbor elevated levels of BCAAs

In mammalian systems, impaired DBT function, as demonstrated by MSUD-affected individuals, results in elevated levels of BCAAs (Kevin A. Strauss and Morton 2003; Chuang, Chuang, and Wynn 2006; Chuang, D. T., Wynn, R. M. and Shih, V. E. 2008). Because *dbt* is disrupted in *que* mutants, I investigated their free amino acid profiles. Owing to the small size of larval zebrafish, a homogenate of 50 whole animals was used for each assay. I compared the free amino acid levels of wild-type and *que* mutant larvae at 96 hpf. Strikingly, *que* larvae harbor elevated levels of BCAAs (Figure 4.3A,B). Isoleucine, leucine and valine concentrations were 788%, 1006% and 688% (n=3, P<0.01) of those of wild-type, respectively. *que* mutants also showed a marked decrease in free glutamine levels, at 24% of wild-type (n=3, P<0.01). In addition, statistically significant decreases were observed in the levels of a wide variety of free amino acids, including aspartate (16%), GABA (32%) and serine (28% of wild-type; all n=3, P<0.01); and alanine (44%), glutamate (38%), glycine (41%), methionine (49%) and threonine (60% of wild-type; all n=3, P<0.05). To rule out the possibility that abnormal motor behavior itself alters free amino acid levels, I examined *beo* mutants, which contain a mutation in the glycine receptor β 2 subunit and exhibit abnormal behavior similar to *que* mutants (Figure 4.3C) (Hirata et al. 2005). The free amino acid levels in *beo* mutants (n=1) were similar to that of wild-type controls, indicating that accordion

behavior alone does not substantially alter free amino acid concentrations. Combined, these data provide strong evidence that mutation of the *que* gene results in an error in amino acid metabolism, yielding a prominent accumulation of BCAAs.

4.4.3 Glutamate levels are reduced in the brain of *que* mutant larvae

Although the neuropathology of MSUD is not well understood, reduced concentrations of neurotransmitters, including glutamate, were observed in the intermediate MSUD mouse model (Zinnanti et al. 2009). Neurotransmitter depletion was found to correlate with abnormal motor behavior and a highly abnormal posture consisting of recumbency and stiff, extended limbs. Given that our analysis of the free amino acids levels in *que* mutants showed decreased concentrations of free glutamate and these mutants demonstrate abnormal CNS function and motor behavior, I examined the distribution of glutamate using an antibody recognizing glutamate and tested it in zebrafish. As a control for antibody penetration and overall tissue morphology, I also stained acetylated tubulin using an acetylated tubulin antibody. Antibody penetration and general morphology of the brain of *que* mutants seemed similar to wild-type at 96 hpf (compare Figure 4.4 A with D). By contrast, glutamate levels were markedly reduced in *que* mutant larvae (n=5 embryos, 12 sections, $P < 0.01$; compare B with E; G). In wild-type larvae an increase of glutamate is observed during development (Figure 4.5A-D). At 96 hpf glutamate is found both in the periphery as well as in the spinal cord (Figure 4.5D). In the mutant *dbt* seems to be mostly absent (Figure 4.5E-H) which probably contributes to the abnormal nervous system function and behavior observed by this stage of development.

4.4.4 The working model

The findings from this study, as well as observations in rodent and human systems, suggest a model for how mutation of the zebrafish *dbt* gene leads to abnormal swimming. In mammalian systems, *dbt* is required for the second step of BCAA metabolism, and its impairment leads to elevated levels of BCAAs and α -keto acids in plasma and tissue (Chuang, Chuang, and Wynn 2006; Chuang, D. T., Wynn, R. M. and Shih, V. E. 2008). Elevated BCAAs in the plasma, in particular leucine, are thought to out-compete other amino acids at the blood-brain barrier, which results in neurotransmitter deficiencies, growth restrictions, cytotoxic edema, myelin disruption, and impaired energy metabolism throughout the CNS (Zinnanti et al. 2009). α -keto acid toxicity has also been proposed to directly disrupt CNS function. Intracranial injection of α -ketovaleric acid, which is derived from valine, has been shown to elicit seizures in rats, whereas administration of other α -keto acids had no behavioral effect (Coitinho et al. 2001). In individuals with MSUD, reducing the concentrations of BCAAs and α -keto acids in the plasma by liver transplantation can protect CNS function and development (K A Strauss et al. 2006).

I propose that very similar mechanisms regulate BCAA metabolism in zebrafish (Figure 4.6). Throughout the first 5 days of zebrafish development, the embryo consumes the presumptive equivalent of a high-protein diet in mammals by absorbing BCAA containing proteins from the yolk (Link, Shevchenko, and Heisenberg 2006; Tay et al. 2006). During the earliest stages of development, within the first few hours post-fertilization, the metabolic needs of the embryo are largely met by maternally derived mitochondria and mRNA (Mendelsohn and Gitlin 2008; Zhang et al. 2008; Abrams and

Mullins 2009). However, as embryogenesis proceeds, BCAA metabolism increasingly relies upon zygotic transcription. In wild-type embryos, BCKD complex function in the liver, other gut organs and the brain itself protect the CNS from BCAA toxicity, similar to mammalian systems. According to this model, BCKD complex function supports appropriate import of amino acids across cerebral barriers, robust metabolic generation of neurotransmitters, which are essential to support the coordinated CNS output that generates vigorous swimming behavior. In *que* mutants, our data indicate that mutation of *dbt* disrupts BCKD complex function to cause the toxic accumulation of BCAAs and probably α -keto acids. This error would cause abnormal retention due to insufficient removal capacities, import of amino acids into the CNS, reduced levels of glutamate and other neurotransmitters, abnormal CNS function leading to accordion behavior (Figure 4.6). It will be interesting to use transgenic approaches to determine whether restoring gene function in the liver of *que* mutants preserves normal CNS function, as shown in mammals (K A Strauss et al. 2006; Kristen J Skvorak, Hager, et al. 2009; Kristen J Skvorak, Paul, et al. 2009). Driving gene expression in other organs not yet explored in mammals can also be investigated, which might indicate new therapeutic options for individuals with MSUD.

4.4.5 Pharmacological evaluation of the working model

The mutation in the *dbt* gene in *que* mutants affects *dbt* protein expression (Figure 3.3), free amino acid and glutamate levels (Figure 4.2) and leads to abnormal CNS output (Figure 2.3) and impaired swimming (Figure 2.1). The mechanism behind these results is not yet fully understood. It is still unclear whether there is one dominant part of the cascade such as the glutamate reduction that is the key factor or if multiple factors, such

as the toxicity of the BCAAs, their keto-acids in addition to a lack of neurotransmitter and neurodegeneration cause the observed phenotype. *que* mutants as a vertebrate model for MSUD could be a powerful tool to answer these questions with but it is still unknown how results obtained using *que* mutants relate to established models and humans.

I therefore performed a pilot drug screen using metabolites known to be upregulated in *que* mutants such as BCAAs and their keto-acids, therapeutics currently used to treat MSUD such as thiamine and phenylbutyrate and compensatory compounds such as nor-leucine thought to compete with leucine and glutamine as a precursor for glutamate which has not yet been proposed as useful drug for MSUD treatment (Table 4.1). Whole wild-type and *que* clutches were incubated at 24 hpf until 96 hpf when time trial analysis was performed. While almost all larvae in the 4mm test were able to finish the task roughly 25% in *que* mutant clutches failed and either failed to leave the inner circle (paralyzed, p) or failed to connect with the 4mm mark (impaired, I) (Figure 4.8A, B). At the highest concentration with less than 15% lethality none of the drugs had an effect on wild-type swimming speeds (Table 4.1; Figure 4.8 G). When applied to *que* clutches phenylbutyrate (Figure 4.8 C) and α -keto- β -methylvaleric acid (KMV) (Figure 4.8D) improved the average swimming speed of the swimming fraction of the clutch. This effect is considered to be mainly affecting the heterozygote larvae since drug application had no effect on wild-types and still roughly 25% don't complete the task which most likely represents the homozygous mutant fraction. To determine whether drug application affects the distribution of swimming performance categories in *que* mutant clutches I performed a X^2 -test (Figure 4.8H). While KMV did not alter the distribution significantly, α -ketoisocaproic acid (KIC) treated clutches had a higher

percentage of paralyzed larvae while application of glutamine and phenylbutyrate slightly reduced this fraction.

4.5 Significance

que larvae harbor a mutation in zebrafish *dbt*, which results in elevated BCAA levels, similar to both the mouse models of MSUD and affected humans. In the mouse model of intermediate MSUD, elevated levels of BCAAs have been shown to correlate with progressive disruption of CNS function and concomitant defects in motor behavior that culminate in severe dystonia (Silberman, Dancis, and Feigin 1961; Morton et al. 2002; Zinnanti et al. 2009). Similarly, severe dystonia has been reported in MSUD-affected individuals during acute metabolic decompensation (Silberman, Dancis, and Feigin 1961; Morton et al. 2002; Zinnanti et al. 2009). *que* mutants demonstrate a progressive defect in motor behavior that culminates in abnormal CNS function and accordion behavior. Accordion behavior is probably the expression of severe dystonia in developing zebrafish. The Downes Lab and others have previously shown that zebrafish mutants that exhibit accordion behavior contain mutations in genes known to control movement and muscle tone in mammalian systems (Downes and Granato 2004; Gleason et al. 2004; Hirata et al. 2005; M. Wang, Wen, and Brehm 2008; Olson, Sgourdou, and Downes 2010).

The findings from this study indicate that *que* mutants are a new animal model of MSUD. One aspect of MSUD is the distinct, maple syrup smell of bodily secretions of affected individuals. I did not detect any distinct odor of *que* mutants (data not shown); however, this is probably due to the small size and minute amounts of secretions

produced by larval zebrafish. Nevertheless, *que* larvae seem to recapitulate molecular, biochemical, cellular and behavioral aspects of MSUD. Because larval zebrafish contain a smaller nervous system than do mammalian systems, with fewer numbers of cells, *que* mutants provide a promising system to better characterize the progression of CNS injury in response to BCAA toxicity. Moreover, the small size, aquatic nature, development that is external to the mother and the ability to obtain large numbers of zebrafish embryos make them amenable to small-molecule screens (Zon and Peterson, 2010). The behavioral phenotype of *que* mutants is robust, easily quantifiable and can respond to known MSUD therapeutics (Figure 4.8); therefore, *que* mutants could be developed into a high throughput system to screen libraries of compounds to identify small molecules that improve swimming behavior. Compounds that improve the behavioral phenotype of *que* mutants could be candidate therapeutics for individuals with MSUD.

Other aspects of MSUD can also be investigated using larval zebrafish. Gene targeting approaches can be readily employed, such as morpholino injection or TALEN technology, to model MSUD caused by disruption of other BCKD complex subunits (Cade et al. 2012; Moore et al. 2012). These technologies can also be used to examine the in vivo role of BCKD regulatory proteins, such as the BCKD phosphatase or kinase. Genetic modifier screens can also be performed using the *que* mutant to search for genes that can compensate for disruptions in BCAA metabolism. Taken together, these approaches can provide a promising platform to better understand CNS metabolism and develop new therapies to combat MSUD.

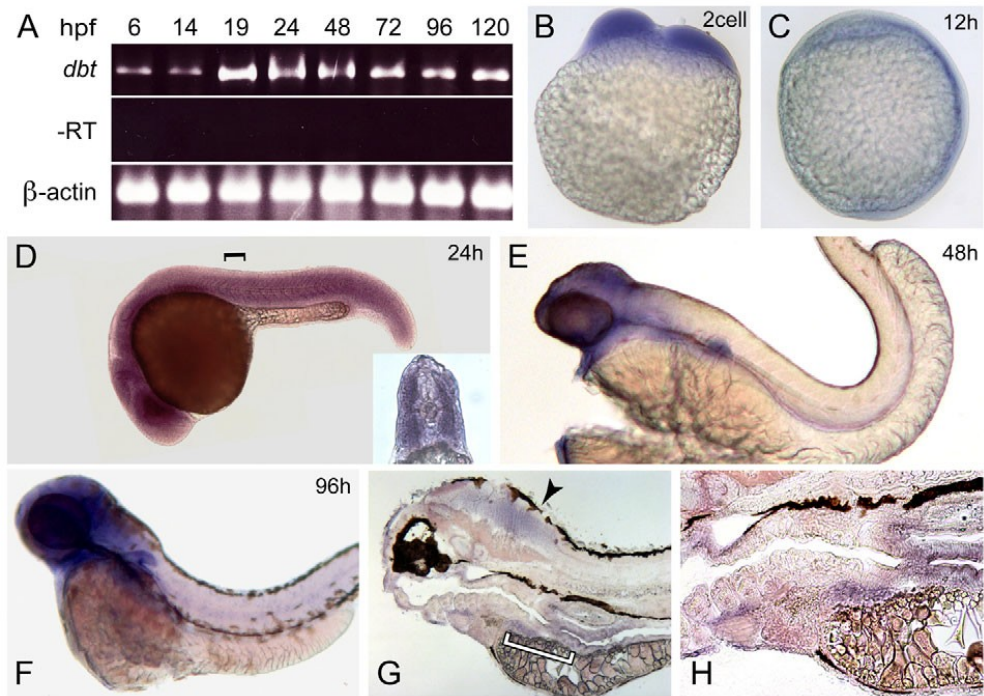


Figure 4.1: *dbt* becomes enriched in the brain and organs in the gut across development

(A) RT-PCR results are shown using mRNA isolated at different time points during zebrafish development. *dbt* was detected at all stages examined. -RT and β -actin controls are also shown. (B-H) In situ hybridization shows broad *dbt* expression at (B) the two-cell stage, (C) 12 hpf and (D) 24 hpf. The inset of a cross section (the black bracket indicates the approximate level of the cross-section) reveals robust *dbt* expression in muscle. *dbt* expression become enriched in the brain and gut at (E) 48 hpf and (F) 96 hpf. (G) Sagittal sections of stained 96 hpf embryos illustrate expression in the brain (arrowhead) and gut. The white bracket indicates a portion of the region shown at higher magnification in H. Above the left edge of the white bracket, *dbt* expression in the liver can be observed, whereas above the right edge of the white bracket, *dbt* expression in the intestine is revealed.

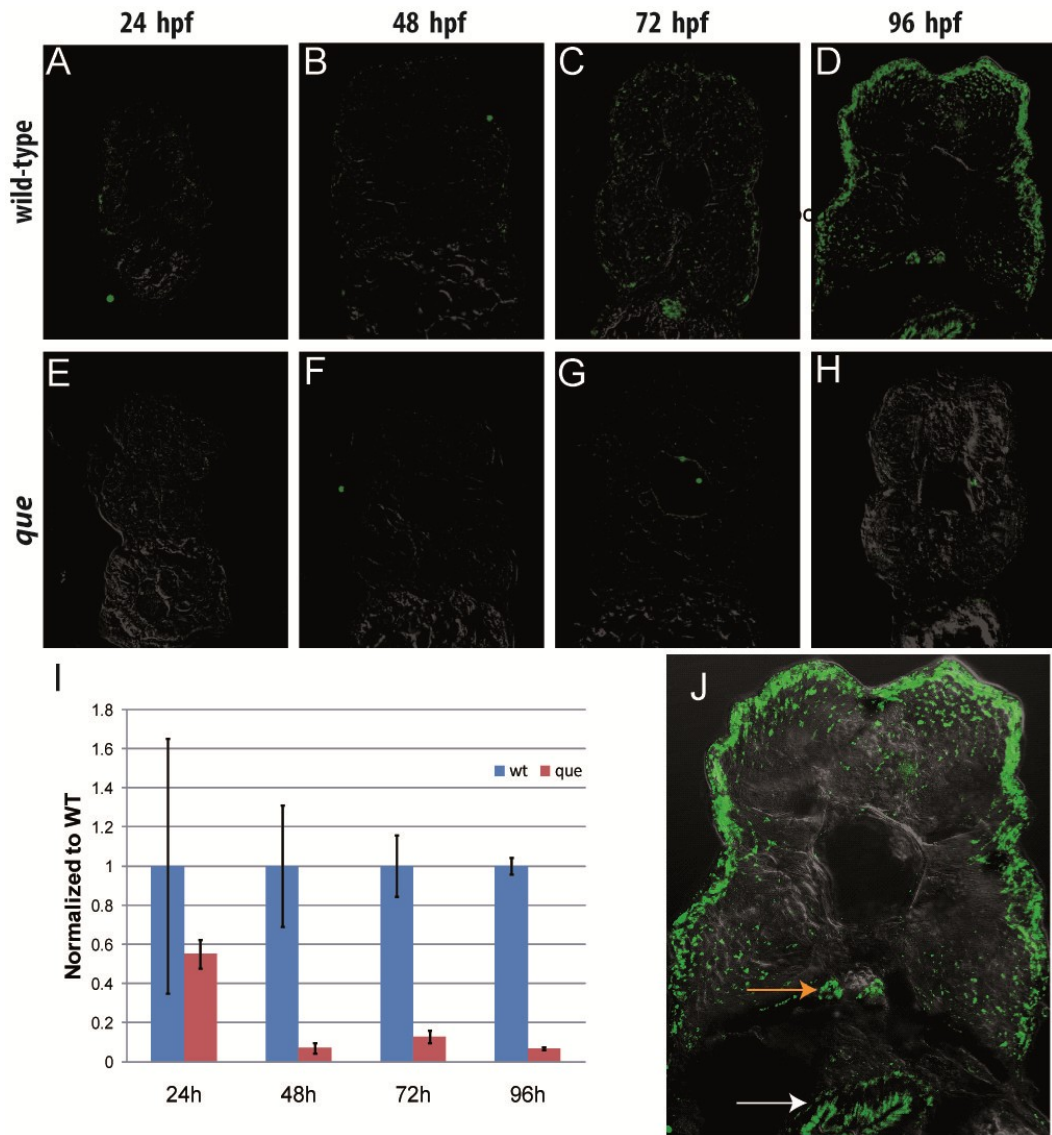


Figure 4.2: *dbt* protein expression during development

Antibody staining on cross sections using an anti-DBT antibody (green) over bright field images. (A-D) in wild-type *dbt* expression increases after 72 hpf and is increased in peripheral structures such as fast muscle fibers, the gut (J, white arrow) and pronephric ducts (J orange arrow). (E-H) in the *que* mutant the *dbt* antibody epitope is mostly absent throughout development. (I) Comparison of *dbt* levels over development based on ROI fluorescence intensity of all tissue dorsal of the yolk. n=2 embryos.

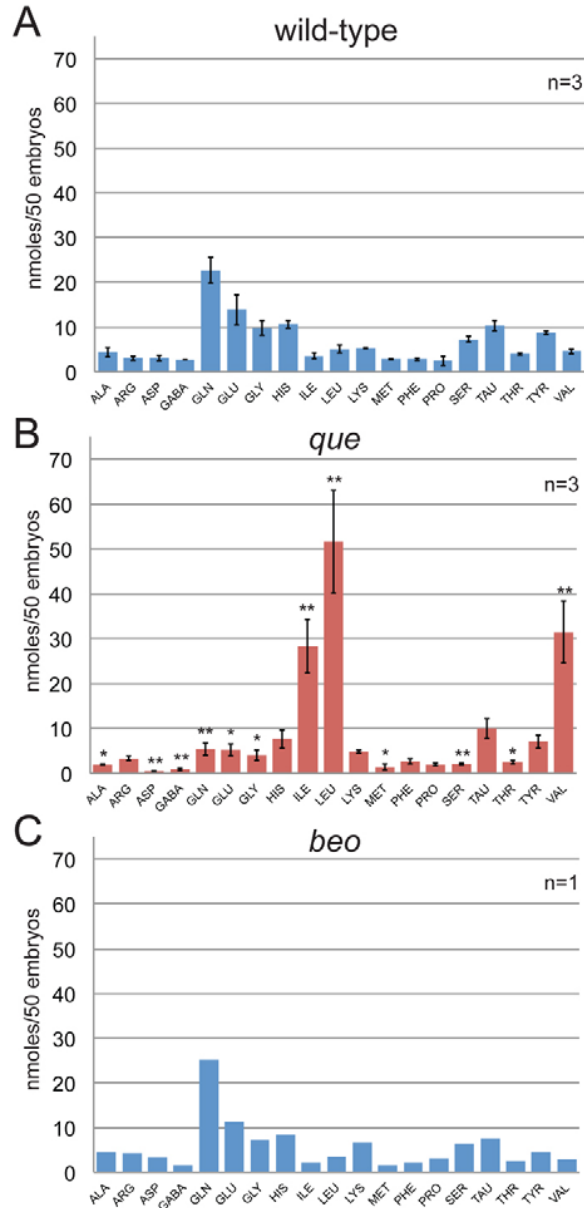


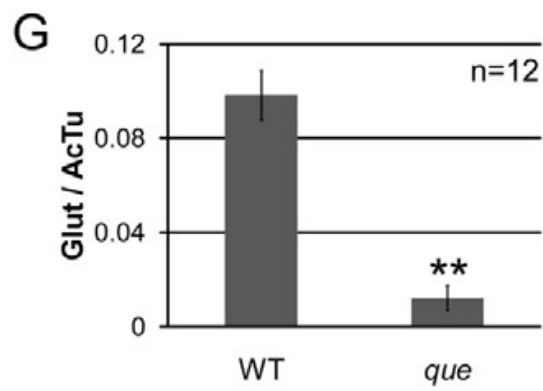
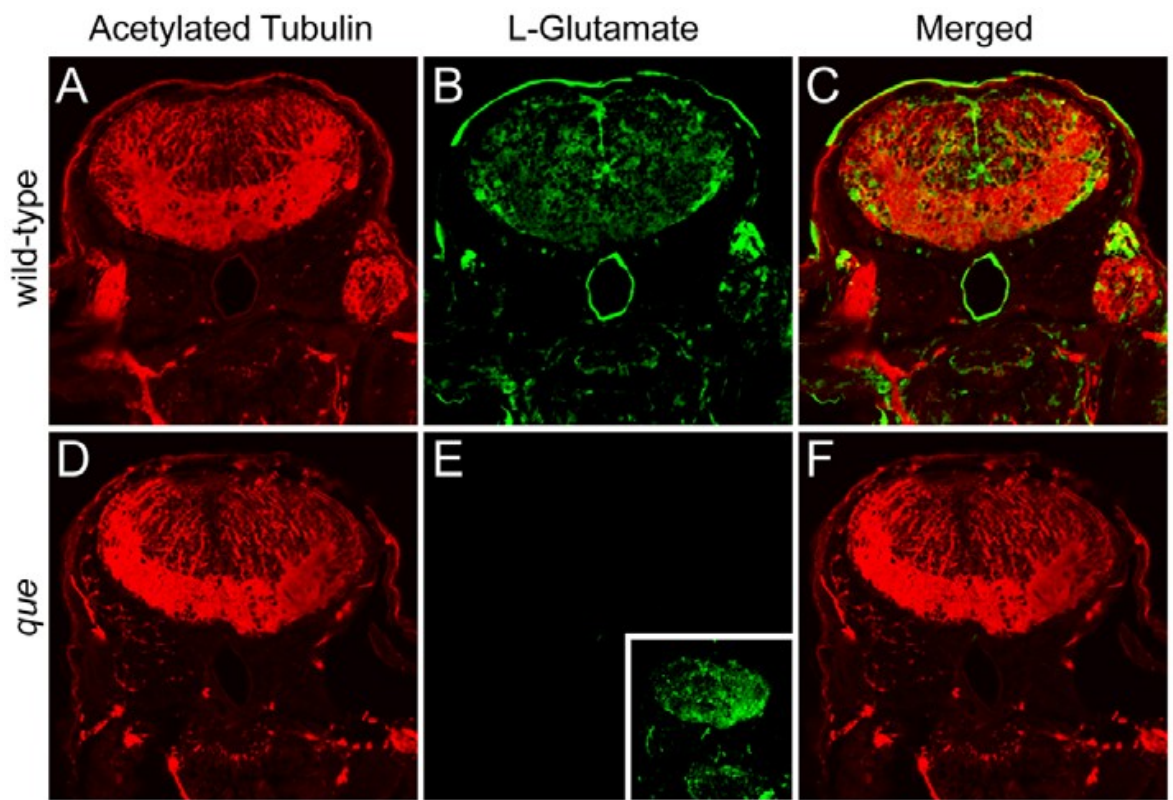
Figure 4.3: The free amino acid profile of *que* mutants shows elevated levels of BCAAs at 96 hpf

The amino acids are referred to by their three-letter code, except for GABA. Each experiment contained a homogenate of 50 larvae. The error bars indicate standard error.

(A) The free amino acid profile for wild-type larvae (n=3). (B) The free amino acid profile of *que* mutant larvae reveals a dramatic accumulation of BCAAs: isoleucine, leucine and valine. Other amino acid levels were reduced. * Significant difference from wild-type at P<0.05; ** significant difference from wild-type at P<0.01 (n=3). (C) The free amino acid profile of *beo*, a zebrafish mutant that demonstrates abnormal behavior owing to a CNS defect, indicates that abnormal behavior alone does not markedly alter free amino acid levels (n=1).

Figure 4.4: *que* mutants contain a reduced concentration of glutamate in the brain.

(A-F) Cross-sectional views of the hind-brain of 96 hpf larvae are shown. Immunohistochemistry using antibodies against acetylated tubulin, which predominantly labels axon tracts, reveals the overall structure of the brain and demonstrates tissue penetration of the antibodies. Staining using an antibody against L-glutamate illustrates the distribution of this neurotransmitter. (A) Labeling with the anti-acetylated tubulin reveals the axon tracts and overall structure of the hind-brain of wild-type larvae. (B) The hind-brain of wild-type larvae contains a broad distribution of L-glutamate. (C) The merged images show several L-glutamate-positive cells surrounded by anti-acetylated tubulin labeling. (D) The overall structure of the hind-brain of *que* mutants revealed by anti-acetylated tubulin appears similar to the hind-brain wild-type larvae. (E) The fluorescence intensity of labeling with the L-glutamate antibody is greatly reduced compared with wild-type when imaged using the same microscope settings. However, increasing the gain of the confocal microscope shows more reduced L-glutamate staining (inset). (F) The merged images show little L-glutamate staining compared with acetylated tubulin labeling. (G) The graph shows a significant reduction in L-glutamate staining intensity in *que* mutants normalized to acetylated tubulin staining. The fluorescent intensity values are the analog-to-digital converter values of the entire frame (n=5 embryos, 12 sections, **P<0.01). Very similar results were obtained when a region of interest was selected to encompass a smaller, designated portion of the brain.



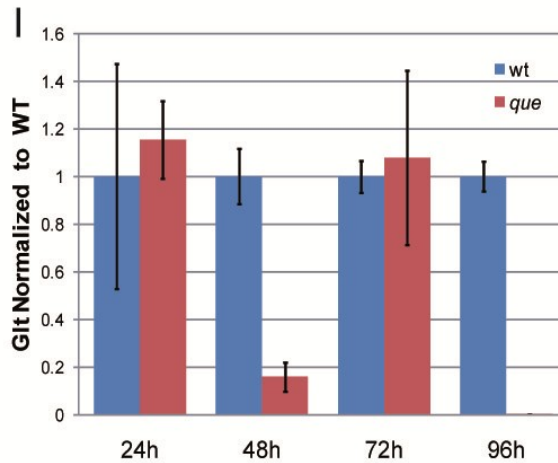
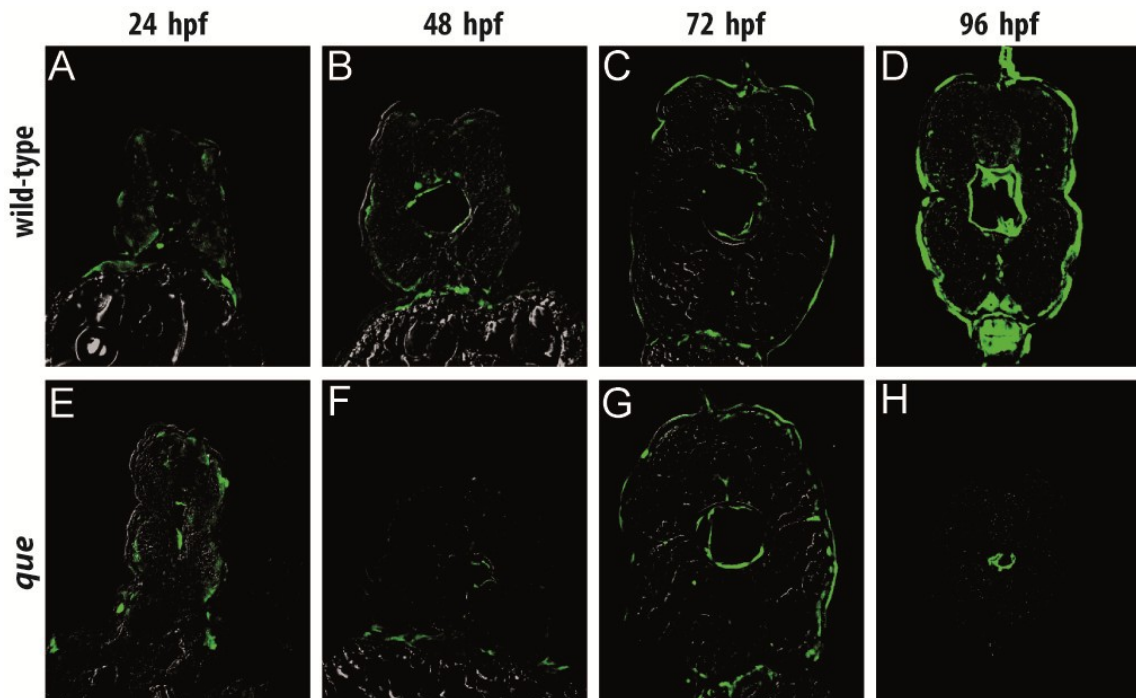


Figure 4.5: Levels of Glutamate during development

Antibody staining on cross sections using an anti-glutamate antibody (green) over bright field images. (A-D) in wild-type glutamate seems to be present in both peripheral areas as well as in the spinal cord throughout development. (E-H) in the *que* mutant glutamate levels vary during development and seem to be reduced at 96 hpf (H) Comparison of glutamate levels over development based on ROI fluorescence intensity of all tissue dorsal of the yolk. n=2 embryos for 24-48 hpf; n=4 embryos for 72 hpf, n=6 for 96 hpf.

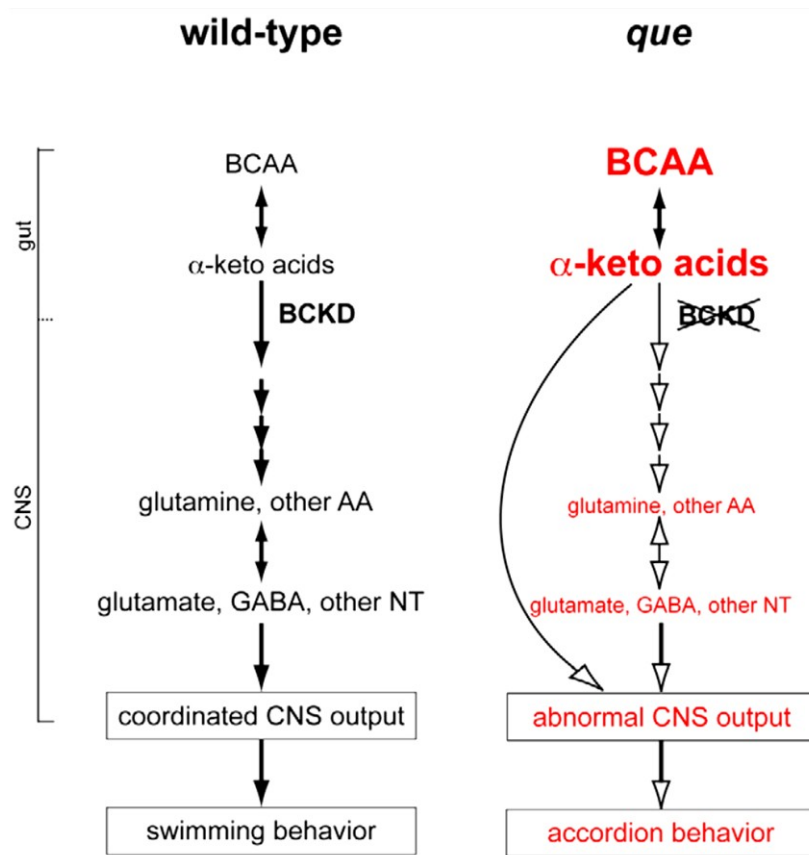


Figure 4.6: A working model of how mutation of *dbt* results in abnormal, accordion behavior

Similar to mammalian systems, I propose that wild-type zebrafish regulate metabolism of BCAAs via the BCKD complex. Many of these metabolic or molecular steps (black arrows) might occur in organs in the gut (such as the liver and intestine) but also the CNS. Amino acids (AA), such as glutamine, are transported across the blood-brain barrier and used to generate glutamate, GABA and other neurotransmitters (NT). These neurotransmitters are required for coordinated nervous system output to orchestrate swimming behavior. In *que* mutants, I propose that impaired BCKD function results in the accumulation of BCAA and α -keto acids. This yields reduced retention and metabolism, and reduced transport of other amino acids (white arrows) across the blood-brain barrier, resulting in diminished neurotransmitter synthesis. The abnormal levels of neurotransmitters contribute to aberrant nervous system output and abnormal, accordion behavior. It is also possible that elevated concentrations of α -keto acids directly disrupt neural circuits to cause accordion behavior.

Compound	Exp. Effect (+/-)	Concentration (mM)
leucine	—	75
valine	—	10
isoleucine	—	2
KMV (α-keto-β-methylvaleric acid)	—	2
KIC (α-ketoisocaproic acid)	—	5
KIV (α-ketoisovaleric acid)	—	10
norleucine	+	40
thiamine	+	1
sodium phenylbutyrate	+	0.01
glutamine	+	0.4

Table 4.1: Compounds and concentrations used for pharmacological pilot screen

For a small pilot screen 10 small compounds were chosen consisting of BCAAs, their keto-acids, drugs currently used in clinical trials and glutamine suggested to be beneficial based on previous results. Their expected effect is noted as well as the highest concentration found to result in less than 15% mortality in wild-type.

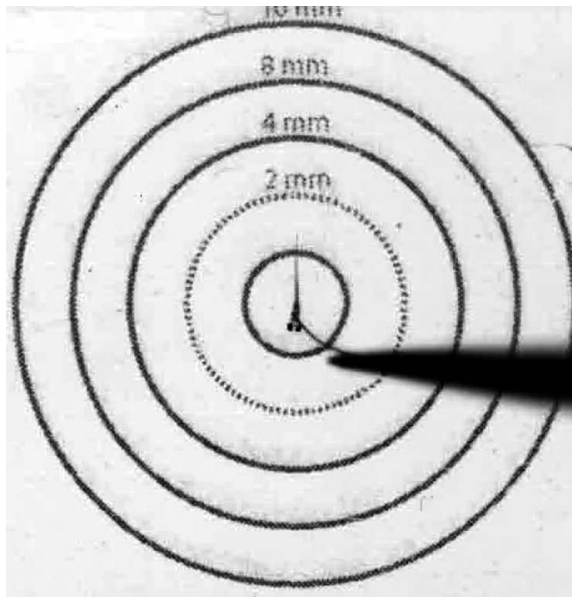


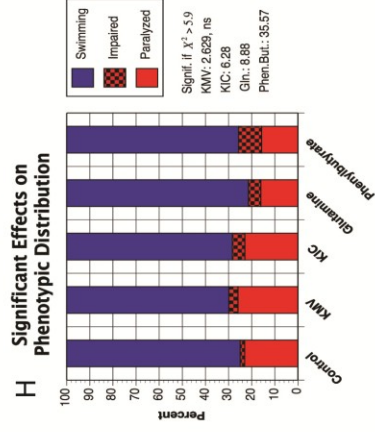
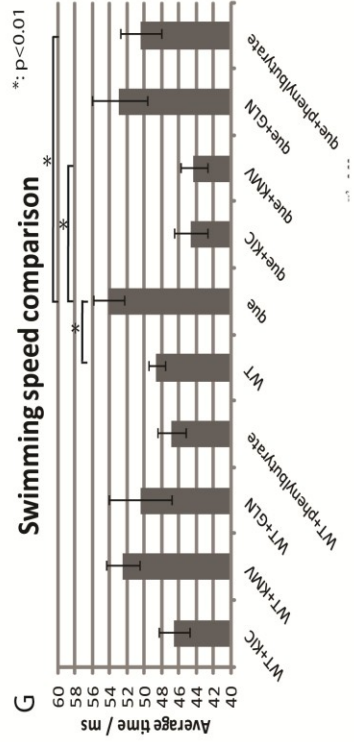
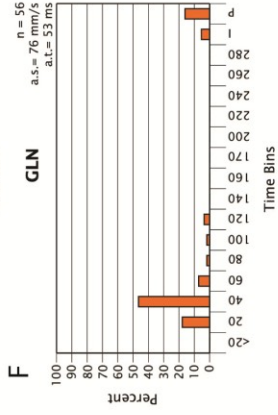
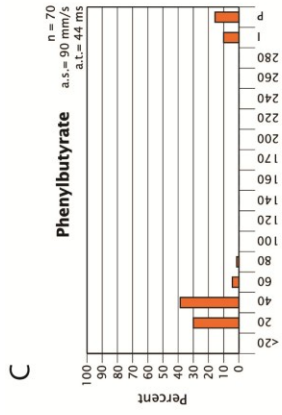
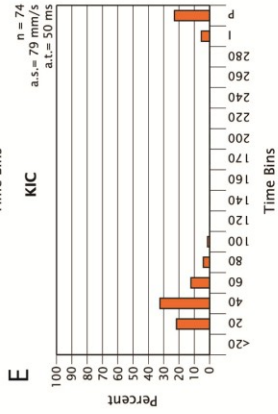
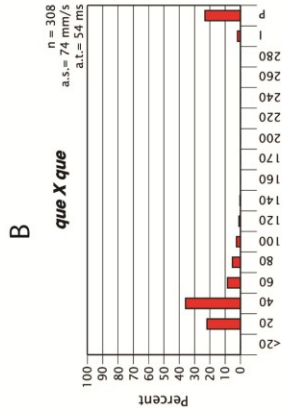
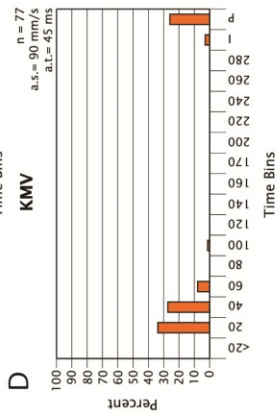
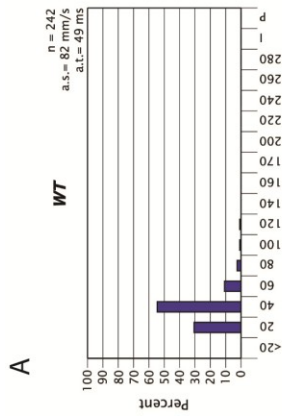
Figure 4.7: Bull's Eye for kinematic analysis

Larvae were placed in the middle of the inner circle. A touch stimulus was applied and the time measured between leaving the inner circle and reaching the 4mm mark.

Figure 4.8: Pharmacological evaluation of the model

Comparison of swimming speeds of whole clutches after drug application. Percentage of the clutch swimming 4mm per time bin. I:percentage of fish leaving the inner circle. P: paralyzed percentage. Embryo numbers, average swimming speed and time given in the upper right corner. (C-F) *que* mutant clutch swimming speeds after drug application. (G)

Comparison of swimming speeds; KMV and phenylbutyrate treatment increases swimming speeds in *que* mutant clutches. (H) χ^2 -analysis; while KIC slightly increases the percentage of larvae unable to perform the task, glutamine and phenylbutyrate improve the swimming performance of that fraction.



CHAPTER 5

SUMMARY AND FUTURE DIRECTIONS

We used the zebrafish motility mutant *que* for the purpose of finding a new gene and molecular event required for locomotion. Since it was unclear at the beginning of this work whether *que* mutants harbor a CNS or muscle related defect I characterized its behavior and showed, that it is similar to both, known muscle and CNS mutants. Wild-type larvae respond to touch with a C-bend and alternating body bends at 96 hpf while *que* mutants fail to perform C-bends and display rostrocaudal shortening instead followed by uncoordinated body bends. To rule out obvious structural defects I used immunohistochemistry and stained fast muscle fibers, sensory and motor neurons but observed no severe structural defects in morphology or distribution. To answer the question whether *que* mutants have a CNS defect we used peripheral nerve recordings to show that the amount of left-right overlap of bursts is significantly increased in the mutant in addition to an increase of swimming bouts. These findings are consistent with the hypothesis that the phenotype in *que* mutants is at least partly caused by abnormal CNS output.

I used meiotic mapping to locate the mutation in *que* mutants to a 0.36cM interval on chromosome 22. The most promising candidate gene of the interval, dihydrolipoamide branched chain transacylase E2 (*dbt*) was sequenced and I found a mutation in the splice donor site of Exon 6 leading to integration of the adjacent intron. This intron sequence codes for four stop codons leading to a truncation of the protein by 224 amino acids including the active site which was confirmed by RT-PCR. Injection of a translation

blocking morpholino copied both the phenotype as well as the reduction of *dbt* protein observed in the mutant. These results strongly suggest that *dbt* is the mutated gene in *que* mutants.

I found that *dbt* is expressed throughout early development and gets enriched in the hind brain as well as the gut region and the liver at 96hpf. Since *dbt* is a key component of the BCAA metabolism we quantified free amino acid levels. While BCAA levels were severely elevated we also noticed a strong reduction of neurotransmitters such as GABA and glutamate. To localize this reduction within the embryo I used anti glutamate immunohistochemistry and observed a strong decrease of glutamate in the hindbrain and spinal cord. To further test the pathway leading from the mutation in *dbt* to the observed phenotype we used a pharmacological approach. In this pilot screen we limited ourselves to the key metabolites in the BCAA pathway such as the BCAAs and their keto acids as well as therapeutic drugs currently used in clinical trials such as thiamine, norleucine and phenylbutyrate. In addition previous results showed a reduction of glutamine, a precursor for glutamate, suggesting glutamine as a potential beneficial drug to test. While the results for both BCAAs as well as their keto acids varied, application of glutamine and phenylbutyrate improved aspects of the swimming performance of mutants.

5.1 *que* mutants as a zebrafish model for MSUD

Many aspects and qualities of the *que* mutant make it a good model for MSUD. First, the model system has some extremely useful qualities such as large clutch size, transparency, external development and an aquatic habitat which can facilitate drug

application. Second, the *que* mutant displays a very robust, distinct phenotype at 96 hpf which facilitates sorting and scoring. The phenotype is also quantifiable and can be detected by automated motion tracking software. Unfortunately it is this robust phenotype that can also be challenging since it lacks a dynamic range; experiments relying on improving the phenotype have to overcome the effects of early BCAA accumulation which can be difficult. It is unknown whether developmental defects occur in zebrafish due to BCAA accumulation and it would be difficult for late genetic or pharmacological rescue approaches to compensate for such defects even if at later stages the gene would have been rendered functional. The fact that MSUD patient's mental capacity declines after every metabolic crisis suggests that damage can occur and is in fact accumulative, even if metabolic balance is restored after crisis (Kevin A. Strauss and Morton 2003; Fernstrom 2005).

5.2 Future directions

This thesis provides a new model form MSUD and evaluated its application for therapeutic screens. While we have identified a reduction of neurotransmitter in this zebrafish model the details of what role this reduction of neurotransmitter plays in MSUD has yet to be addressed. The cascade of events leading from the accumulation of BCAAs to the observed phenotype is still unknown.

5.2.1 The role of Glutamate and neurotransmitter reduction

The observed neurotransmitter reduction could be the cause for the observed phenotype. One way to test this hypothesis would be to replenish or at least elevate glutamate levels in the *que* mutant. We attempted this by making use of the

technotrousers (*tnt*) mutant which has a mutation in the glial glutamate transporter *slc1a2b* (McKeown et al. 2012). If a lack of glutamate is indeed causing the phenotype then blocking the glial glutamate transporter in *que* mutants should increase synaptic glutamate and might restore the swimming capability of *que* mutants. In this first attempt *que* mutants injected with a morpholino knocking down *slc1a2b* failed to show increased performance in time trial assays (control injected *que* clutch: 20% phenotype, n=40; *slc1a2* MO injected *que* clutch: 57% phenotype, n=30). I also tried the reverse experiment and injected *tnt* mutants with the *dbt* morpholino and also saw no significant effect on their performance (control injected *tnt* mutants: 92% phenotype, n=23; *slc1a2b* MO injected *tnt* mutants: 84% phenotype, n=30). There are several possibilities to explain this outcome. First, it could have been, that we didn't elevate or decrease glutamate levels enough to overcome the loss of glutamate in *que* mutants or decrease the glutamate levels effectively in *tnt* mutants. Second, there are other key effects, unaddressed by focusing on glutamate alone. We found that GABA levels are also reduced. And patients are known to have a reduction of dopamine, norepinephrine, aspartate among other neurotransmitters and precursors (Kevin A. Strauss and Morton 2003; Zinnanti et al. 2009; Zinnanti and Lazovic 2012).

5.2.2 Screening for therapeutic compounds

The pilot screen confirmed beneficial effects of phenylbutyrate and glutamine. These results are encouraging and suggest that further evaluation can be performed to develop *que* mutants as a large-scale drug screening tool. A pitfall for expanding screens is the difficulty of having a quantifiable output that is still in a dynamic range of the spectrum of measurements. The results of our pilot screen indicate that, while the readout

is very robust, the range of results is not dynamic; the changes in swimming speeds or distribution are not yet applicable for a large scale screen.

Two strategies could be considered to overcome this problem. Ideally the behavior as output should remain since it is the behavior that is most striking and a key element in human MSUD patients as well. To establish a dynamic range the morpholino could be used and titrated down to the smallest concentration that still produces the phenotype. At this threshold concentration treatment conditions with beneficial effects have the highest chance to also influence the behavior. Injection experiments are normally rather difficult to incorporate into large scale screens but attempts have been made to automate the process (W. Wang et al. 2007) which could facilitate large-scale experiments. Second, another readout method could be used. Focusing on the glutamate reduction the use of genetic glutamate reporters could be evaluated (Hires, Zhu, and Tsien 2008) to circumvent the need for IHC.

Based on the literature it is unlikely that one compound alone will have the strongest effect. A screen should therefore incorporate conditions of two or more compounds to uncover potential synergistic effects (Kevin A. Strauss and Morton 2003; Chuang, D. T., Wynn, R. M. and Shih, V. E. 2008)

5.2.3 Tissue specific rescue

One way of treating MSUD patients at the moment is a liver transplantation. Unfortunately the supply of donor organs is limited and standby times can be considerably long. Therefore it would be beneficial if other organ suitable for transplantation would also have the same or similar effects which is supported by our

expression data as well as the fact that in rodents *Dbt* is expressed in most tissues (Doering et al. 1998). To pursue the hypothesis that *dbt* expression in other organs such as kidney, stomach and muscle tissue, general rescue need to be demonstrated as well as tissue specific expression. We attempted the first step towards this aim, general rescue, through several approaches. I injected *dbt* transcript into mutant clutches at the 1-4 cell stage and quantified the swimming performance at 96 hpf. This failed to improve swimming performance. A likely possibility is that the turnover rate of the RNA reduces the effects of RNA injection at 96 hpf. We tried to overcome this problem by injecting a DNA construct with SV40 driving *dbt*. It too failed to improve swimming performance most likely due to the diluting factor and the choice of the promoter which sometimes induces only minimal expression in zebrafish. A construct with CMV driving *dbt* flanked by TOL2 sites for genome integration when coinjected with transposase was generated but failed to improve the behavioral phenotype. We tested if injected mutants would have increased *dbt* protein using western blot analysis and found that *dbt* levels were still reduced and comparable to those of uninjected mutants. Sequencing of the CMV promoter revealed a sequence alteration which could potentially have reduced expression of the construct. The same construct with a β -actin promoter is currently being tested.

After having found a robust rescue strategy the promoter could be swapped with a tissue specific promoter driving *dbt* only in one tissue. This approach would not only allow spatial control but coupled with conditional gene control such as tet-on system (Knopf et al. 2010) could provide temporal control to generate juvenile or adult mutants. Such mutants could be used to investigate the mechanisms of acute metabolic crises at adult stages, simulating metabolic crises as encountered by many MSUD patients.

5.2.4 The pathway from BCAAs to the phenotype

In this thesis we showed that the mutation in *dbt* causes elevated BCAA levels. We also observed reduced levels of neurotransmitters and an abnormal CNS output. It is unlikely that the model shown in Figure 4.6 represents all aspects both in the linear sequence as well as in the multitude of potential parallel pathways influencing the CNS and the behavior.

We observed expression of *dbt* in the hindbrain. While the CPG circuitry is situated in the spinal cord and by itself sufficient to perform escape responses, the CPG could be modulated by abnormal firing patterns in the hindbrain of *que* mutants. To distinguish whether or not edemas or other neuronal abnormalities in the hindbrain influence CPG function, the head region could be lesioned off and the touch response analyzed at 96 hpf. While an outcome with no change would not rule out a pre-lesioned influence of the hindbrain, a change in the response could indicate an influence of the hindbrain on the CPG in mutants.

Zebrafish also offers the possibility of targeting other components of this pathway. Morpholino knockdown and TALEN technology allow to reduce expression or terminate expression of other components of the BCKD complex. An interesting first target is the E3 subunit since it is involved in both pyruvate dehydrogenase and α -ketoglutarate dehydrogenase complexes in addition to the BCKD complex.

APPENDIX

A MACONDO CRUDE OIL FROM THE DEEPWATER HORIZON OIL SPILL DISRUPTS SPECIFIC DEVELOPMENTAL PROCESSES DURING ZEBRAFISH EMBRYOGENESIS

This addition was modified from a joint publication based on a collaboration with Michael Barresi and colleagues (de Soysa et al. 2012).

The Deepwater Horizon disaster was the largest marine oil spill in history, and total vertical exposure of oil to the water column suggests it could impact an enormous diversity of ecosystems. The most vulnerable organisms are those encountering these pollutants during their early life stages. Water-soluble components of crude oil and specific polycyclic aromatic hydrocarbons have been shown to cause defects in cardiovascular and craniofacial development in a variety of teleost species, but the developmental origins of these defects have yet to be determined. We asked whether water accumulated fractions (WAF) of the Deepwater Horizon oil could impact specific embryonic developmental processes. While not a native species to the Gulf waters, the developmental biology of zebrafish has been well characterized and makes it a powerful model system to reveal the cellular and molecular mechanisms behind Macondo crude toxicity. Here we show significant response reduction and abnormal escape responses in developing zebrafish in response to WAF exposure.

A.1 Methods

A. 1. 1 Behavioral analysis

In an effort to perform a more conservative assessment of locomotor behavior, analysis was carried out using a 50% WAF solution. Embryos exposed to either 50% or 100% WAF had similar locomotor responses (data not shown). To characterize larval swimming behavior at 48 hpf, a light touch stimulus was applied to the head of larvae. The minimum stimulus required to elicit a response was determined using pressure specific Von Frey filaments. The touch-response was recorded using a high-speed camera (Fastec Imaging, San Diego, CA, USA) at 1,000 frames per second (fps). A 35 mm lens (Nikon, Melville, NY, USA) was used for magnification. To illustrate the responses, single frames taken at 20 ms intervals were overlaid in Adobe Photoshop (San Jose, CA, USA). For kinematic analysis, the head-to-tail angles were calculated for each frame using automated software developed by the Downes Lab (Biology Department, University of Massachusetts, Amherst, MA, USA) (Downes and Granato 2006). In brief, pixel density was used to identify three landmarks along the larval body: the tip of the nose, the border between the yolk extension, and the tip of the tail. These three points form an angle, which was plotted over time using Microsoft Excel (Microsoft Corporation, Redmond, WA, USA). To calculate body bend frequency, a full body bend was defined as two intervals of more than 50 degrees of opposite directions. To determine the duration of a swimming episode, we measured the beginning of a swimming episode until the final time the body was straightened to within 20 degrees of being straight (defined as 0 degrees).

A.1.2 Locomotor behavior

During our many WAF treatments it was clearly evident embryos displayed irregular swimming behaviors. The locomotor escape response to stimuli is an important survival behavior that develops later in embryogenesis. Interestingly, previous studies examining the effect of PAHs on zebrafish swimming behavior did not reveal any significant phenotypes (Incardona, Collier, and Scholz 2004). Therefore, we systematically tested whether exposure to Macondo crude oil WAF impacted swimming patterns and escape responses. To do this, we recorded the swimming behavior of individual 48 hpf larvae with a high-speed video camera (1,000 frames/second) following the administration of a specific touch stimulus (Burgess and Granato 2007). WAF-treated embryos demonstrated abnormal swimming behavior and a failure to escape based on multiple criteria. WAF-treated embryos showed reduced sensitivity to touch stimuli, as demonstrated by 70% response rate for WAF-treated embryos as compared to a 99% response rate for untreated control embryos (n = 100 trials from 10 embryos each). When a response was produced in WAF-treated embryos they showed a significantly reduced frequency of body bends (Control, 39.10Hz; WAF, 18.82Hz; n = 10 each; t-test, P <0.01) and swam for less time than untreated control embryos (Control, 875.8ms; WAF, 282ms; n = 10 each; t-test, P = 0.01) (Figure A.1). The presence of locomotor behavior phenotypes suggests that there could either be a problem with neural transmission or a developmental problem resulting from an anatomical deformation in the nervous or musculature systems.

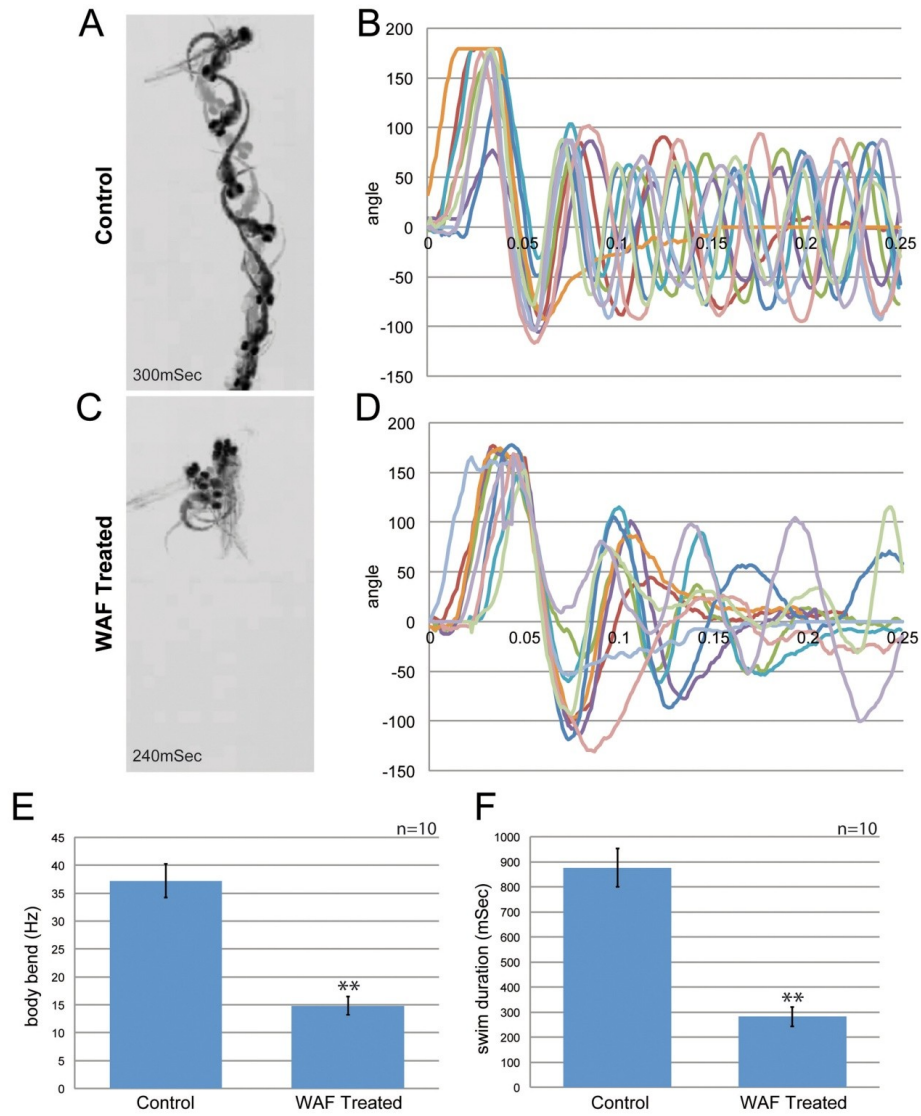


Figure A.1: Macondo crude oil exposure impaired escape behavior by 48 hpf

(A) Individual frames from high-speed video recordings are shown for control larvae. The images are overlaid in 20 ms intervals and the duration of the response captured within the field is indicated. (B) Kinematics traces are shown for 10 escape responses each for control larvae. 0° indicates a straight body and positive and negative angles represent body bends in opposite directions. The time is indicated in seconds. (C) Image overlays for a WAF-treated larva escape response illustrate the failure to clear the field that was frequently observed. (D) Kinematic traces for WAF-treated larvae reveal reduced, abnormal body bend frequencies. (E) Quantification of body bend frequencies. (F) Quantification of the duration of escape responses reveals that WAF-treated larvae respond for shorter periods of time. Asterisks in E and F indicate statistically significant differences ($n = 10$, $P < 0.01$).

REFERENCES

- Abrams, Elliott W, and Mary C Mullins. 2009. "Early Zebrafish Development: It's in the Maternal Genes." *Current Opinion in Genetics & Development* 19 (4) (August): 396–403. doi:10.1016/j.gde.2009.06.002.
- Amsterdam, A, S Burgess, G Golling, W Chen, Z Sun, K Townsend, S Farrington, M Haldi, and N Hopkins. 1999. "A Large-scale Insertional Mutagenesis Screen in Zebrafish." *Genes & Development* 13 (20) (October 15): 2713–2724.
- Baraban, Scott C, Matthew T Dinday, Peter A Castro, Sally Chege, Stephan Guyenet, and Michael R Taylor. 2007. "A Large-scale Mutagenesis Screen to Identify Seizure-resistant Zebrafish." *Epilepsia* 48 (6) (June): 1151–1157. doi:10.1111/j.1528-1167.2007.01075.x.
- Bill, Brent R, Andrew M Petzold, Karl J Clark, Lisa A Schimmenti, and Stephen C Ekker. 2009. "A Primer for Morpholino Use in Zebrafish." *Zebrafish* 6 (1) (March): 69–77. doi:10.1089/zeb.2008.0555.
- Burgess, Harold A, and Michael Granato. 2007. "Sensorimotor Gating in Larval Zebrafish." *The Journal of Neuroscience: The Official Journal of the Society for Neuroscience* 27 (18) (May 2): 4984–4994. doi:10.1523/JNEUROSCI.0615-07.2007.
- Buss, R R, and P Drapeau. 2001. "Synaptic Drive to Motor neurons During Fictive Swimming in the Developing Zebrafish." *Journal of Neurophysiology* 86 (1) (July): 197–210.
- Cade, Lindsay, Deepak Reyon, Woong Y Hwang, Shengdar Q Tsai, Samir Patel, Cyd Khayter, J Keith Joung, Jeffry D Sander, Randall T Peterson, and Jing-Ruey Joanna Yeh. 2012. "Highly Efficient Generation of Heritable Zebrafish Gene Mutations Using Homo- and Heterodimeric TALENs." *Nucleic Acids Research* (June 7). doi:10.1093/nar/gks518. <http://www.ncbi.nlm.nih.gov/pubmed/22684503>.
- Calingasan, N Y, D J Ho, E J Wille, M V Campagna, J Ruan, M Dumont, L Yang, Q Shi, G E Gibson, and M F Beal. 2008. "Influence of Mitochondrial Enzyme Deficiency on Adult Neurogenesis in Mouse Models of Neurodegenerative Diseases." *Neuroscience* 153 (4) (June 2): 986–996. doi:10.1016/j.neuroscience.2008.02.071.
- Chuang, David T, Jacinta L Chuang, and R Max Wynn. 2006. "Lessons from Genetic Disorders of Branched-chain Amino Acid Metabolism." *The Journal of Nutrition* 136 (1 Suppl) (January): 243S–9S.
- Chuang, D. T., Wynn, R. M. and Shih, V. E. 2008. *The Online Metabolic And Molecular Bases Of Inherited Diseases*. 2008th ed. New York: McGraw-Hill.
- Coitinho, A S, C F de Mello, T T Lima, J de Bastiani, M R Figuera, and M Wajner. 2001. "Pharmacological Evidence That Alpha-ketoisovaleric Acid Induces Convulsions Through GABAergic and Glutamatergic Mechanisms in Rats." *Brain Research* 894 (1) (March 9): 68–73.

- Danner, D J, N Armstrong, S C Heffelfinger, E T Sewell, J H Priest, and L J Elsas. 1985. "Absence of Branched Chain Acyl-transferase as a Cause of Maple Syrup Urine Disease." *The Journal of Clinical Investigation* 75 (3) (March): 858–860. doi:10.1172/JCI111783.
- Danner, D J, and C B Doering. 1998. "Human Mutations Affecting Branched Chain Alpha-ketoacid Dehydrogenase." *Frontiers in Bioscience: a Journal and Virtual Library* 3 (June 3): d517–524.
- Dodd, P R, S H Williams, A L Gundlach, P A Harper, P J Healy, J A Dennis, and G A Johnston. 1992. "Glutamate and Gamma-aminobutyric Acid Neurotransmitter Systems in the Acute Phase of Maple Syrup Urine Disease and Citrullinemia Encephalopathies in Newborn Calves." *Journal of Neurochemistry* 59 (2) (August): 582–590.
- Doering, C B, C Coursey, W Spangler, and D J Danner. 1998. "Murine Branched Chain Alpha-ketoacid Dehydrogenase Kinase; cDNA Cloning, Tissue Distribution, and Temporal Expression During Embryonic Development." *Gene* 212 (2) (June 8): 213–219.
- Downes, Gerald B, and Michael Granato. 2004. "Acetylcholinesterase Function Is Dispensable for Sensory Neurite Growth but Is Critical for Neuromuscular Synapse Stability." *Developmental Biology* 270 (1) (June 1): 232–245. doi:10.1016/j.ydbio.2004.02.027.
- . 2006. "Supraspinal Input Is Dispensable to Generate Glycine-mediated Locomotive Behaviors in the Zebrafish Embryo." *Journal of Neurobiology* 66 (5) (April): 437–451. doi:10.1002/neu.20226.
- Drapeau, P, D W Ali, R R Buss, and L Saint-Amant. 1999. "In Vivo Recording from Identifiable Neurons of the Locomotor Network in the Developing Zebrafish." *Journal of Neuroscience Methods* 88 (1) (April 1): 1–13.
- Eaton, R C, R D Farley, C B Kimmel, and E Schabtach. 1977. "Functional Development in the Mauthner Cell System of Embryos and Larvae of the Zebra Fish." *Journal of Neurobiology* 8 (2) (March): 151–172. doi:10.1002/neu.480080207.
- Fernhoff, P M, D Lubitz, D J Danner, P P Dembure, H P Schwartz, R Hillman, D M Bier, and L J Elsas. 1985. "Thiamine Response in Maple Syrup Urine Disease." *Pediatric Research* 19 (10) (October): 1011–1016. doi:10.1203/00006450-198510000-00012.
- Fernstrom, John D. 2005. "Branched-chain Amino Acids and Brain Function." *The Journal of Nutrition* 135 (6 Suppl) (June): 1539S–46S.
- Fisher, C W, K S Lau, C R Fisher, R M Wynn, R P Cox, and D T Chuang. 1991. "A 17-bp Insertion and a Phe215----Cys Missense Mutation in the Dihydrolipoyl Transacylase (E2) mRNA from a Thiamine-responsive Maple Syrup Urine Disease Patient WG-34." *Biochemical and Biophysical Research Communications* 174 (2) (January 31): 804–809.
- Friedrich, Timo, Aaron M Lambert, Mark A Masino, and Gerald B Downes. 2012. "Mutation of Zebrafish Dihydrolipoamide Branched-chain Transacylase E2 Results in

- Motor Dysfunction and Models Maple Syrup Urine Disease.” *Disease Models & Mechanisms* 5 (2) (March): 248–258. doi:10.1242/dmm.008383.
- Funchal, Cláudia, Aline Meyer Rosa, Moacir Wajner, Susana Wofchuk, and Regina Pessoa Pureur. 2004. “Reduction of Glutamate Uptake into Cerebral Cortex of Developing Rats by the Branched-chain Alpha-keto Acids Accumulating in Maple Syrup Urine Disease.” *Neurochemical Research* 29 (4) (April): 747–753.
- Geisler, Robert, Gerd-Jörg Rauch, Silke Geiger-Rudolph, Andrea Albrecht, Frauke van Bebber, Andrea Berger, Elisabeth Busch-Nentwich, et al. 2007. “Large-scale Mapping of Mutations Affecting Zebrafish Development.” *BMC Genomics* 8: 11. doi:10.1186/1471-2164-8-11.
- Gleason, Michelle R, Ricardo Armisen, Mark A Verdecia, Howard Sirotkin, Paul Brehm, and Gail Mandel. 2004. “A Mutation in *Serca* Underlies Motility Dysfunction in Accordion Zebrafish.” *Developmental Biology* 276 (2) (December 15): 441–451. doi:10.1016/j.ydbio.2004.09.008.
- Granato, M, F J van Eeden, U Schach, T Trowe, M Brand, M Furutani-Seiki, P Haffter, et al. 1996. “Genes Controlling and Mediating Locomotion Behavior of the Zebrafish Embryo and Larva.” *Development (Cambridge, England)* 123 (December): 399–413.
- Haffter, P, M Granato, M Brand, M C Mullins, M Hammerschmidt, D A Kane, J Odenthal, et al. 1996. “The Identification of Genes with Unique and Essential Functions in the Development of the Zebrafish, *Danio Rerio*.” *Development (Cambridge, England)* 123 (December): 1–36.
- Hao, Jijun, Charles H Williams, Morgan E Webb, and Charles C Hong. 2010. “Large Scale Zebrafish-based in Vivo Small Molecule Screen.” *Journal of Visualized Experiments: JoVE* (46). doi:10.3791/2243. <http://www.ncbi.nlm.nih.gov/pubmed/21248690>.
- Harper, P A, J A Dennis, P J Healy, and G K Brown. 1989. “Maple Syrup Urine Disease in Calves: a Clinical, Pathological and Biochemical Study.” *Australian Veterinary Journal* 66 (2) (February): 46–49.
- Herring, W J, M McKean, N Dracopoli, and D J Danner. 1992. “Branched Chain Acyltransferase Absence Due to an Alu-based Genomic Deletion Allele and an Exon Skipping Allele in a Compound Heterozygote Proband Expressing Maple Syrup Urine Disease.” *Biochimica Et Biophysica Acta* 1138 (3) (March 20): 236–242.
- Hirata, Hiromi, Louis Saint-Amant, Gerald B Downes, Wilson W Cui, Weibin Zhou, Michael Granato, and John Y Kuwada. 2005. “Zebrafish Bandoneon Mutants Display Behavioral Defects Due to a Mutation in the Glycine Receptor Beta-subunit.” *Proceedings of the National Academy of Sciences of the United States of America* 102 (23) (June 7): 8345–8350. doi:10.1073/pnas.0500862102.
- Hirata, Hiromi, Louis Saint-Amant, Julie Waterbury, Wilson Cui, Weibin Zhou, Qin Li, Daniel Goldman, Michael Granato, and John Y Kuwada. 2004. “Accordion, a Zebrafish

Behavioral Mutant, Has a Muscle Relaxation Defect Due to a Mutation in the ATPase Ca²⁺ Pump SERCA1.” *Development (Cambridge, England)* 131 (21) (November): 5457–5468. doi:10.1242/dev.01410.

Hires, Samuel Andrew, Yongling Zhu, and Roger Y. Tsien. 2008. “Optical Measurement of Synaptic Glutamate Spillover and Reuptake by Linker Optimized Glutamate-sensitive Fluorescent Reporters.” *Proceedings of the National Academy of Sciences* 105 (11) (March 18): 4411–4416. doi:10.1073/pnas.0712008105.

Homanics, Gregg E, Kristen Skvorak, Carolyn Ferguson, Simon Watkins, and Harbhajan S Paul. 2006. “Production and Characterization of Murine Models of Classic and Intermediate Maple Syrup Urine Disease.” *BMC Medical Genetics* 7: 33. doi:10.1186/1471-2350-7-33.

Incardona, John P, Tracy K Collier, and Nathaniel L Scholz. 2004. “Defects in Cardiac Function Precede Morphological Abnormalities in Fish Embryos Exposed to Polycyclic Aromatic Hydrocarbons.” *Toxicology and Applied Pharmacology* 196 (2) (April 15): 191–205. doi:10.1016/j.taap.2003.11.026.

Klivenyi, Peter, Anatoly A Starkov, Noel Y Calingasan, Gabrielle Gardian, Susan E Browne, Lichuan Yang, Parvesh Bubber, Gary E Gibson, Mulchand S Patel, and M Flint Beal. 2004. “Mice Deficient in Dihydrolipoamide Dehydrogenase Show Increased Vulnerability to MPTP, Malonate and 3-nitropropionic Acid Neurotoxicity.” *Journal of Neurochemistry* 88 (6) (March): 1352–1360.

Knerr, Ina, Natalie Weinhold, Jerry Vockley, and K Michael Gibson. 2012. “Advances and Challenges in the Treatment of Branched-chain Amino/keto Acid Metabolic Defects.” *Journal of Inherited Metabolic Disease* 35 (1) (January): 29–40. doi:10.1007/s10545-010-9269-1.

Knopf, Franziska, Kristin Schnabel, Christa Haase, Katja Pfeifer, Konstantinos Anastassiadis, and Gilbert Weidinger. 2010. “Dually Inducible TetON Systems for Tissue-specific Conditional Gene Expression in Zebrafish.” *Proceedings of the National Academy of Sciences* 107 (46) (November 16): 19933–19938. doi:10.1073/pnas.1007799107.

Langenbacher, Adam D, Catherine T Nguyen, Ann M Cavanaugh, Jie Huang, Fei Lu, and Jau-Nian Chen. 2011. “The PAF1 Complex Differentially Regulates Cardiomyocyte Specification.” *Developmental Biology* 353 (1) (May 1): 19–28. doi:10.1016/j.ydbio.2011.02.011.

Lefebvre, Julie L, Fumihito Ono, Cristina Puglielli, Glen Seidner, Clara Franzini-Armstrong, Paul Brehm, and Michael Granato. 2004. “Increased Neuromuscular Activity Causes Axonal Defects and Muscular Degeneration.” *Development (Cambridge, England)* 131 (11) (June): 2605–2618. doi:10.1242/dev.01123.

Legendre, P, and H Korn. 1994. “Glycinergic Inhibitory Synaptic Currents and Related Receptor Channels in the Zebrafish Brain.” *The European Journal of Neuroscience* 6 (10) (October 1): 1544–1557.

- Link, Vinzenz, Andrej Shevchenko, and Carl-Philipp Heisenberg. 2006. "Proteomics of Early Zebrafish Embryos." *BMC Developmental Biology* 6: 1. doi:10.1186/1471-213X-6-1.
- Mackenzie, D Y, and L I Woolf. 1959. "Maple Syrup Urine Disease; an Inborn Error of the Metabolism of Valine, Leucine, and Isoleucine Associated with Gross Mental Deficiency." *British Medical Journal* 1 (5114) (January 10): 90–91.
- Masino, Mark A, and Joseph R Fetcho. 2005. "Fictive Swimming Motor Patterns in Wild Type and Mutant Larval Zebrafish." *Journal of Neurophysiology* 93 (6) (June): 3177–3188. doi:10.1152/jn.01248.2004.
- McKeown, Kelly Anne, Rosa Moreno, Victoria L Hall, Angeles B Ribera, and Gerald B Downes. 2012. "Disruption of *Eaat2b*, a Glutamate Transporter, Results in Abnormal Motor Behaviors in Developing Zebrafish." *Developmental Biology* 362 (2) (February 15): 162–171. doi:10.1016/j.ydbio.2011.11.001.
- Mendelsohn, Bryce A, and Jonathan D Gitlin. 2008. "Coordination of Development and Metabolism in the Pre-midblastula Transition Zebrafish Embryo." *Developmental Dynamics: An Official Publication of the American Association of Anatomists* 237 (7) (July): 1789–1798. doi:10.1002/dvdy.21584.
- Moore, Finola E, Deepak Reyon, Jeffry D Sander, Sarah A Martinez, Jessica S Blackburn, Cyd Khayter, Cherie L Ramirez, J Keith Joung, and David M Langenau. 2012. "Improved Somatic Mutagenesis in Zebrafish Using Transcription Activator-Like Effector Nucleases (TALENs)." *PloS One* 7 (5): e37877. doi:10.1371/journal.pone.0037877.
- Morton, D Holmes, Kevin A Strauss, Donna L Robinson, Erik G Puffenberger, and Richard I Kelley. 2002. "Diagnosis and Treatment of Maple Syrup Disease: a Study of 36 Patients." *Pediatrics* 109 (6) (June): 999–1008.
- Ogier de Baulny, H, and J M Saudubray. 2002. "Branched-chain Organic Acidurias." *Seminars in Neonatology: SN* 7 (1) (February): 65–74. doi:10.1053/siny.2001.0087.
- Olson, Bryan D, Paraskevi Sgourdou, and Gerald B Downes. 2010. "Analysis of a Zebrafish Behavioral Mutant Reveals a Dominant Mutation in *atp2a1/SERCA1*." *Genesis (New York, N.Y.: 2000)* 48 (6) (June): 354–361. doi:10.1002/dvg.20631.
- Parng, Chuenlei, Wen Lin Seng, Carlos Semino, and Patricia McGrath. 2002. "Zebrafish: A Preclinical Model for Drug Screening." *ASSAY and Drug Development Technologies* 1 (1) (November): 41–48. doi:10.1089/154065802761001293.
- Pei, Wuhong, Lisa E Kratz, Isa Bernardini, Raman Sood, Tohei Yokogawa, Heidi Dorward, Carla Ciccone, et al. 2010. "A Model of Costeff Syndrome Reveals Metabolic and Protective Functions of Mitochondrial OPA3." *Development (Cambridge, England)* 137 (15) (August 1): 2587–2596. doi:10.1242/dev.043745.

- Saint-Amant, L, and P Drapeau. 1998. "Time Course of the Development of Motor Behaviors in the Zebrafish Embryo." *Journal of Neurobiology* 37 (4) (December): 622–632.
- Salo, Antti M., Helen Cox, Peter Farndon, Celia Moss, Helen Grindulis, Maija Risteli, Simon P. Robins, and Raili Myllylä. 2008. "A Connective Tissue Disorder Caused by Mutations of the Lysyl Hydroxylase 3 Gene." *The American Journal of Human Genetics* 83 (4) (October 10): 495–503. doi:10.1016/j.ajhg.2008.09.004.
- Silberman, J, J Dancis, and I Feigin. 1961. "Neuropathological Observations in Maple Syrup Urine Disease: Branched-chain Ketoaciduria." *Archives of Neurology* 5 (October): 351–363.
- Skvorak, K J. 2009. "Animal Models of Maple Syrup Urine Disease." *Journal of Inherited Metabolic Disease* 32 (2) (April): 229–246. doi:10.1007/s10545-009-1086-z.
- Skvorak, Kristen J, Elizabeth J Hager, Erland Arning, Teodoro Bottiglieri, Harbhajan S Paul, Stephen C Strom, Gregg E Homanics, et al. 2009. "Hepatocyte Transplantation (HTx) Corrects Selected Neurometabolic Abnormalities in Murine Intermediate Maple Syrup Urine Disease (iMSUD)." *Biochimica Et Biophysica Acta* 1792 (10) (October): 1004–1010. doi:10.1016/j.bbadis.2009.08.006.
- Skvorak, Kristen J, Harbhajan S Paul, Kenneth Dorko, Fabio Marongiu, Ewa Ellis, Donald Chace, Carolyn Ferguson, K Michael Gibson, Gregg E Homanics, and Stephen C Strom. 2009. "Hepatocyte Transplantation Improves Phenotype and Extends Survival in a Murine Model of Intermediate Maple Syrup Urine Disease." *Molecular Therapy: The Journal of the American Society of Gene Therapy* 17 (7) (July): 1266–1273. doi:10.1038/mt.2009.99.
- de Soysa, T Yvanka, Allison Ulrich, Timo Friedrich, Danielle Pite, Shannon L Compton, Deborah Ok, Rebecca L Bernardos, et al. 2012. "Macondo Crude Oil from the Deepwater Horizon Oil Spill Disrupts Specific Developmental Processes During Zebrafish Embryogenesis." *BMC Biology* 10 (1) (May 4): 40. doi:10.1186/1741-7007-10-40.
- Strauss, K A, G V Mazariegos, R Sindhi, R Squires, D N Finegold, G Vockley, D L Robinson, et al. 2006. "Elective Liver Transplantation for the Treatment of Classical Maple Syrup Urine Disease." *American Journal of Transplantation: Official Journal of the American Society of Transplantation and the American Society of Transplant Surgeons* 6 (3) (March): 557–564. doi:10.1111/j.1600-6143.2005.01209.x.
- Strauss, Kevin A, Bridget Wardley, Donna Robinson, Christine Hendrickson, Nicholas L Rider, Erik G Puffenberger, Diana Shellmer, Diana Shelmer, Ann B Moser, and D Holmes Morton. 2010. "Classical Maple Syrup Urine Disease and Brain Development: Principles of Management and Formula Design." *Molecular Genetics and Metabolism* 99 (4) (April): 333–345. doi:10.1016/j.ymgme.2009.12.007.
- Strauss, Kevin A., and D. Holmes Morton. 2003. "Branched-chain Ketoacyl Dehydrogenase Deficiency: Maple Syrup Disease." *Current Treatment Options in Neurology* 5 (4) (July): 329–341.

Tay, Tuan Leng, Qingsong Lin, Teck Keong Seow, Keng Hwa Tan, Choy Leong Hew, and Zhiyuan Gong. 2006. "Proteomic Analysis of Protein Profiles During Early Development of the Zebrafish, *Danio Rerio*." *Proteomics* 6 (10) (May): 3176–3188. doi:10.1002/pmic.200600030.

Thisse, Christine, and Bernard Thisse. 2008. "High-resolution in Situ Hybridization to Whole-mount Zebrafish Embryos." *Nature Protocols* 3 (1): 59–69. doi:10.1038/nprot.2007.514.

Tschopp, Markus, Masanari Takamiya, Kara L Cervený, Gaia Gestri, Oliver Biehlmaier, Stephen W Wilson, Uwe Strähle, and Stephan C F Neuhauss. 2010. "Funduscopy in Adult Zebrafish and Its Application to Isolate Mutant Strains with Ocular Defects." *PLoS One* 5 (11): e15427. doi:10.1371/journal.pone.0015427.

Wang, Meng, Hua Wen, and Paul Brehm. 2008. "Function of Neuromuscular Synapses in the Zebrafish Choline-acetyltransferase Mutant *Bajan*." *Journal of Neurophysiology* 100 (4) (October): 1995–2004. doi:10.1152/jn.90517.2008.

Wang, Wenhui, Xinyu Liu, Danielle Gelinás, Brian Ciruna, and Yu Sun. 2007. "A Fully Automated Robotic System for Microinjection of Zebrafish Embryos." *PLoS ONE* 2 (9) (September 12): e862. doi:10.1371/journal.pone.0000862.

Warp, Erica, Gautam Agarwal, Claire Wyart, Drew Friedmann, Claire S Oldfield, Alden Conner, Filippo Del Bene, Aristides B Arrenberg, Herwig Baier, and Ehud Y Isacoff. 2012. "Emergence of Patterned Activity in the Developing Zebrafish Spinal Cord." *Current Biology: CB* 22 (2) (January 24): 93–102. doi:10.1016/j.cub.2011.12.002.

Wolman, Marc, and Michael Granato. 2012. "Behavioral Genetics in Larval Zebrafish: Learning from the Young." *Developmental Neurobiology* 72 (3) (March): 366–372. doi:10.1002/dneu.20872.

Zhang, Yong-Zhong, Ying-Chun Ouyang, Yi Hou, Heide Schatten, Da-Yuan Chen, and Qing-Yuan Sun. 2008. "Mitochondrial Behavior During Oogenesis in Zebrafish: a Confocal Microscopy Analysis." *Development, Growth & Differentiation* 50 (3) (March): 189–201. doi:10.1111/j.1440-169X.2008.00988.x.

Zhong, Hanbing, and Shuo Lin. 2011. "Chemical Screening with Zebrafish Embryos." *Methods in Molecular Biology* (Clifton, N.J.) 716: 193–205. doi:10.1007/978-1-61779-012-6_12.

Zinnanti, William J, and Jelena Lazovic. 2012. "Interrupting the Mechanisms of Brain Injury in a Model of Maple Syrup Urine Disease Encephalopathy." *Journal of Inherited Metabolic Disease* 35 (1) (January): 71–79. doi:10.1007/s10545-011-9333-5.

Zinnanti, William J, Jelena Lazovic, Kathleen Griffin, Kristen J Skvorak, Harbhajan S Paul, Gregg E Homanics, Maria C Bewley, Keith C Cheng, Kathryn F Lanoue, and John M Flanagan. 2009. "Dual Mechanism of Brain Injury and Novel Treatment Strategy in Maple Syrup Urine Disease." *Brain: a Journal of Neurology* 132 (Pt 4) (April): 903–918. doi:10.1093/brain/awp024.

Zon, Leonard I, and Randall Peterson. 2010. "The New Age of Chemical Screening in Zebrafish." *Zebrafish* 7 (1) (March): 1. doi:10.1089/zeb.2010.9996.

Zottoli, Steven J., and Donald S. Faber. 2000. "Review: The Mauthner Cell: What Has It Taught Us?" *The Neuroscientist* 6 (1) (February 1): 26–38. doi:10.1177/107385840000600111.